Tectonophysics 814 (2021) 228970

Contents lists available at ScienceDirect

Tectonophysics

journal homepage: www.elsevier.com/locate/tecto

Mesozoic structural inheritance in the Cenozoic evolution of the central Catalan Coastal Ranges (western Mediterranean): Structural and magnetotelluric analysis in the Gaià-Montmell High

Miquel Marín [a,b,*], Eduard Roca [b], Alex Marcuello [b], Lluís Cabrera [b], Oriol Ferrer [b]

[a] Schlumberger, Aachen Technology Center, Ritterstraβe 23, 52072 Aachen, Germany
[b] Institut de Recerca Geomodels, Departament de Dinàmica de la Terra i de l'Oceà, Universitat de Barcelona, Martí i Franquès s/n, 08028 Barcelona, Spain

ARTICLE INFO

Keywords:
Structural inheritance
Inversion tectonics
Western Mediterranean
Catalan Coastal Ranges
Magnetotellurics
Tectonic evolution

ABSTRACT

The control exerted by the Mesozoic basin configuration on the Cenozoic tectonic evolution of the Catalan Coastal Ranges has been frequently recognized as a key factor to explain its present-day structure. However, details of this structural inheritance and its evolution through geological time is still under discussion. In this work we present two structural cross-sections based on fieldwork, well and magnetotelluric data in order to illustrate the structural styles and tectonic evolution of the Gaià-Montmell High. Here, the Montmell Fault not only constitutes the SW segment of one of the major Neogene faults in the Catalan Coastal Ranges (the Montmell-Vallès Fault System), but also the NW limit of a Late Jurassic-Early Cretaceous extensional basin(the Montmell-Garraf Basin), facts that denote a major role of this fault in the tectonic evolution of the area. The present-day structure of the Gaià-Montmell High resulted, therefore, from two successive episodes of inversion during the Cenozoic. The first one reactivated the Montmell Fault as compressional during the Paleogene. As a result, and among other inversion-related structures, the Gaià-El Camp Thrust developed sa major NW-directed basement footwall shortcut. Later on, the previously formed compressional structure during the Paleogene became reactivated as extensional during the Neogene. During this phase, the reactivation of the Montmell Fault looks limited and, hence, the extension is transmitted to the Baix Penedès Fault. The reactivation of the Gaià-El Camp Thrust is also manifest in the development of an array of extensional faults in the backlimb of the Carme-Cabra Anticline that corresponds to the NE-end of El Camp Fault. This episode of negative inversion developed accommodation zones between the four major faults present in the area (Vallès-Penedès, Montmell, El Camp and Baix Penedès faults) that are characterized by the presence of relay ramps with breaching faults.

1. Introduction

Pre-existing faults and stratigraphic variations commonly play a major role in determining regional evolution during later deformation (Jackson, 1980; Cooper et al., 1989; Williams et al., 1989; Coward, 1994; Buchanan and Buchanan, 1995; Butler et al., 2006). It has been widely described how pre-existing faults control not only the location and kinematics of later structures (i.e., folds and faults) but also the shape and location of orogenic belts and rifts. The structural configuration during the opening of the Bay of Biscay and western Tethys during the Mesozoic has been widely recognized as a key factor that controlled the location and kinematics of the orogenic belts developed in the NE Iberian Peninsula during Late Cretaceous-Cenozoic. Examples of this structural control are found in the Pyrenees (Muñoz, 1992; Bond and McClay, 1995; García-Senz, 2002; Mencos et al., 2015; Muñoz, 2017), the Iberian Chain (Salas and Casas, 1993; Guimerà et al., 1995; Salas et al., 2001; Nebot and Guimerà, 2016; Guimerà, 2018; Aldega et al., 2019), the Columbrets Basin in the Valencia Trough (Etheve et al., 2018; Roma et al., 2018) and the Betic Chain (Calvert et al., 2000; Vergés et al., 2002). Nevertheless, the role played by the Mesozoic structures in the Catalan Intraplate Chain (CIC), an orogenic belt also developed NE of the Iberian Peninsula during the Cenozoic (Guimerà, 1984; Gaspar-Escribano et al., 2004; Juez-Larré and Andriessen, 2006), is not completely understood.

The development of the present-day basin-and-range configuration of the Catalan Coastal Ranges (CCR) (Fig. 1) resulted from the

* Corresponding author at: Schlumberger, Aachen Technology Centre, Ritterstraβe 23, 52072 Aachen, Germany.
E-mail address: mperez92@slb.com (M. Marín).

https://doi.org/10.1016/j.tecto.2021.228970
Received 19 August 2020; Received in revised form 9 June 2021; Accepted 14 June 2021
Available online 17 June 2021

extensional reactivation of the main Paleogene contractional structures (Fontboté, 1954; Gaspar-Escribano et al., 2004; López-Blanco et al., 2000; Marcén et al., 2018). Thus, the presence of pre-existing faults has been considered as a key factor controlling the tectonic evolution of the CCR during the Neogene (Guimerà et al., 1995; Roca et al., 1999; Marín et al., 2008; Baqués et al., 2012).

The control played by pre-Cenozoic structures is still poorly constrained and mostly supported by changes in stratigraphic thicknesses and regional observations (e.g., Esteban and Robles, 1976; Salas and Casas, 1993; Salas et al., 2001). Other studies state the potential Cenozoic reactivation of Mesozoic extensional faults in the region (Roca and Guimerà, 1992; Gómez and Guimerà, 1999) and the control the stratigraphic changes of the Mesozoic succession had in the development of Paleogene contractional structures (Anadón et al., 1985; Guimerà and Álvaro, 1990). Moreover, some works based on geochemical analysis in crustal-scale fault damage zones and gouges (i.e., neoformation of minerals, fluid circulation) reveal multiple reactivations in response to the tectonic phases affecting the Iberian Peninsula since the Mesozoic (e.g., Baqués et al., 2013; Cantarero et al., 2014) and even before the Mesozoic (Marcén et al., 2018; Aldega et al., 2019).

In this paper, we define the structure of a portion of the NW margin of the Montmell-Garraf Basin (Salas, 1987), one of the stratigraphically differentiated rift basins developed in NE Iberian Peninsula Late Jurassic-Early Cretaceous. This area is characterized by the presence of a strip of Paleogene folds and thrusts, located at the southern prolongation of the major Neogene Vallès-Penedès extensional Fault (Fig. 1). The study is essentially focused on the recognition of the main structural features and the description of the role played by the Mesozoic basin architecture during the Cenozoic tectonic evolution.

The work is supported by the construction of two structural cross-sections based on field and well data (Gaià-Montmell and the Marmellar sections, Fig. 2) that allow the delineation of the structures of the uppermost crust. The geometry of the basement and major faults is also sustained at depth by a magnetotelluric (MT) survey carried out along the Gaià-Montmell section, which yields information on the electrical response of the crust up to about 4 km depth.

2. Geological setting

2.1. Tectonic setting

Located in northeastern Iberian Peninsula, the CCR is a structural unit with a NE-SW-oriented basin and range physiography that extends parallel to the coastline for more than 250 km (Fig. 1). It is approximately 30 km wide and, in the present-day, constitutes the onshore expression of the extensional continental margin that separates the thinned crust of the Valencia Trough from the relatively thick crust of the Iberian Plate (Dañobeitia et al., 1992; Roca and Guimerà, 1992;

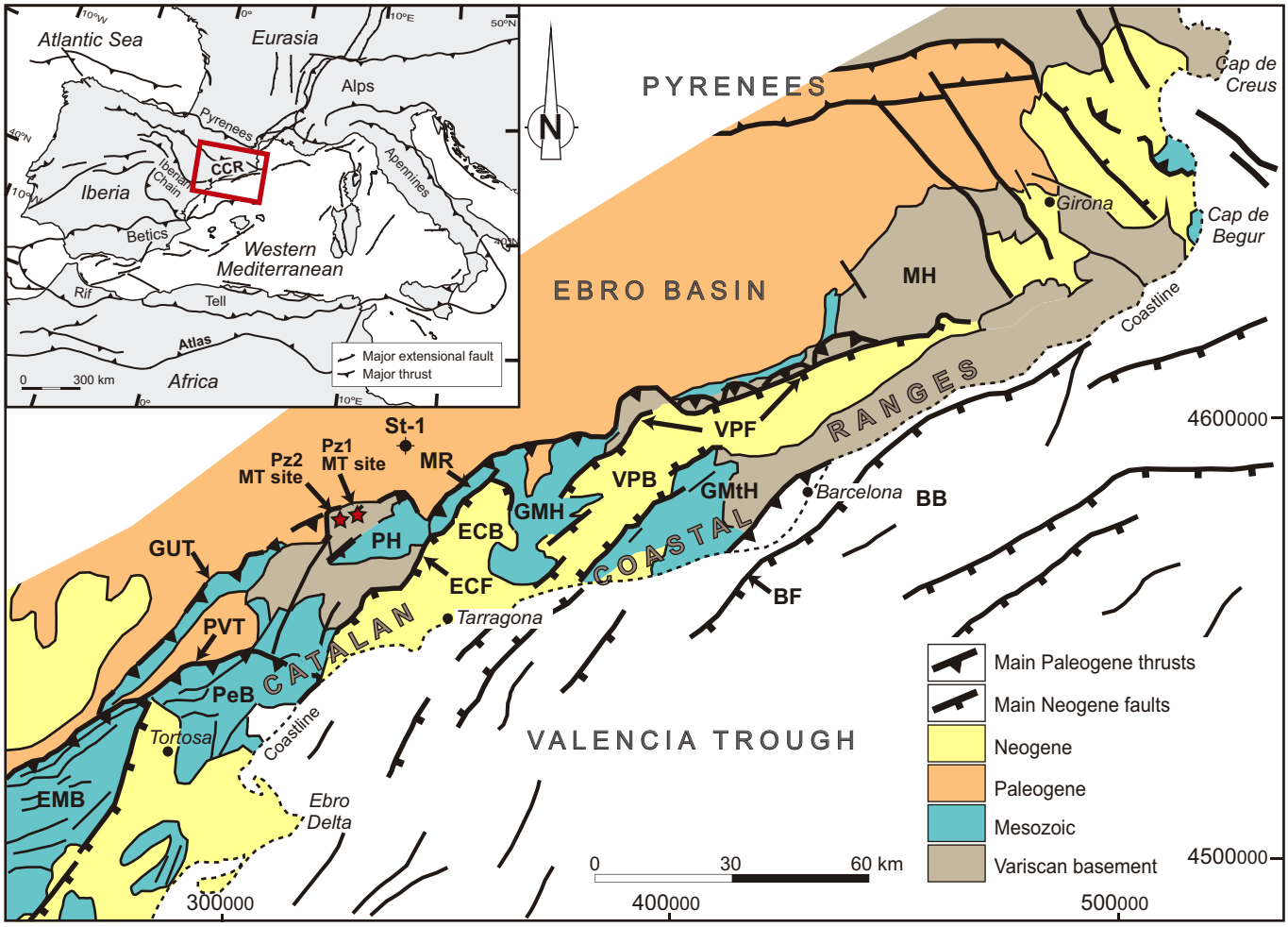

Fig. 1. Schematic structural map of the Catalan Margin (Western Mediterranean). ECB: El Camp Basin; ECF: El Camp Fault; GMtH: Garraf-Montnegre High; GMH: Gaià-Montmell High; MR: Miramar Range; PH: Prades High; VPB: Vallès-Penedès Basin; VPF: Vallès-Penedès Fault; MH: Montseny High; BF: Barcelona Fault; BB: Barcelona Basin; GUT: Gandesa-Ulldemolins Thrust; PVT: Portalrubio-Vandellòs Thrust; PeB: Perelló Mesozoic Basin; EMB: Eastern Maestrat Mesozoic Basin; St-1: Senant-1 well. Red stars in the Prades High indicate the location of the two MT soundings recorded on top of Paleozoic rocks. (For interpretation of the references to color in this figure legend, the reader is referred to the web version of this article.)

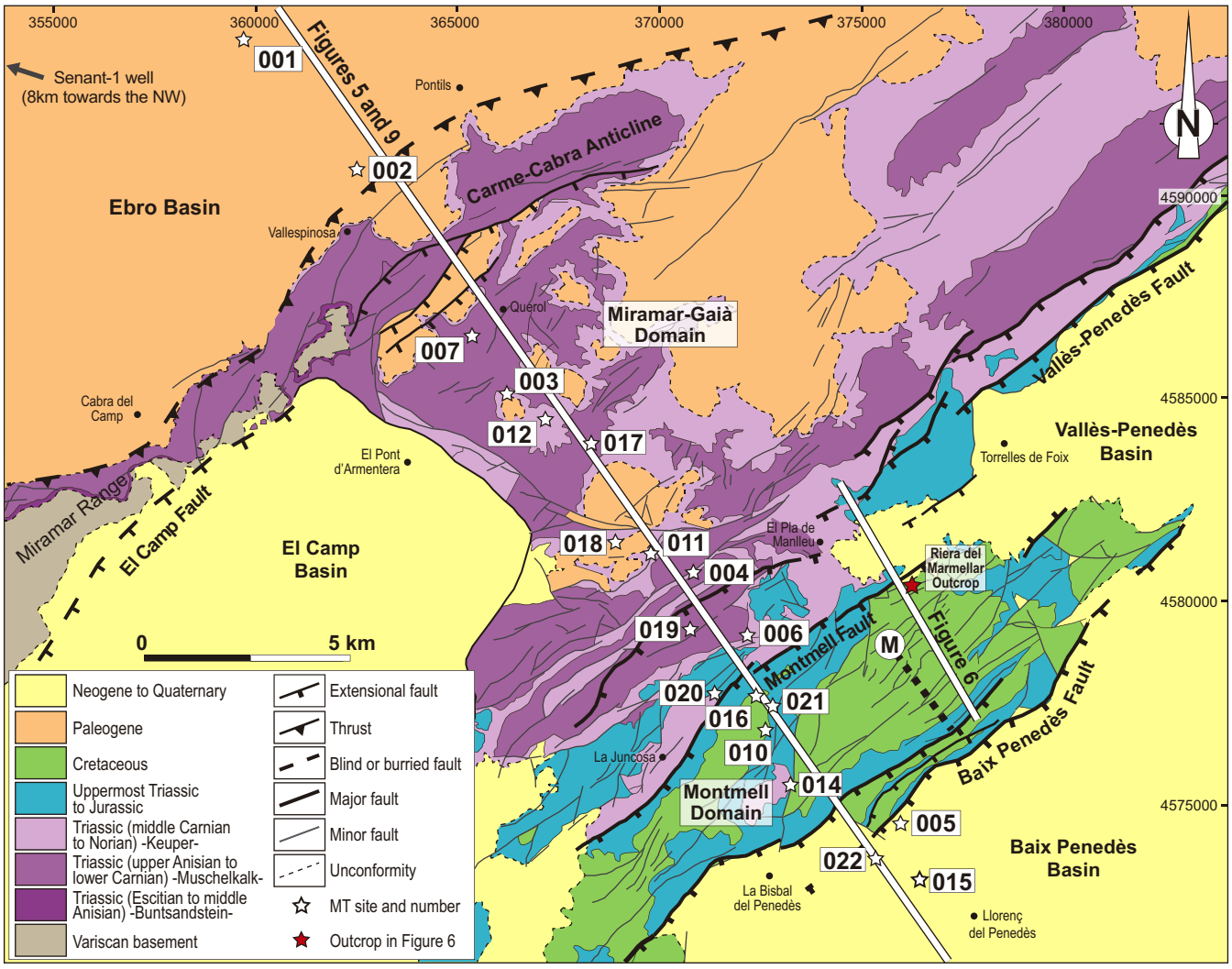

Fig. 2. Geological map of the Gaià-Montmell High and surrounding areas. The map includes the location the Gaià-Montmell and the Marmellar cross-sections (Figs. 5 and 6 respectively) and the acquired parametric MT soundings along the Gaià-Montmell section. M-labelled thick dashed line indicates the aproximate location of the Mesozoic succession-type described by Salas (1987) in the Marmellar area. Black dots are village locations used in the text to facilitat the explanations. See Fig. 1 for the exact location of the Senant-1 well.

Vidal et al., 1995). The CCR is formed by several ENE- to NE-striking basement blocks bounded by 50 to 150 km-long faults that display a right-stepping *en-echelon* arrangement (Fig. 1). These major faults mostly dip towards the SE and show reverse, normal and limited left-lateral strike-slip motion (Ashauer and Teichmüller, 1935; Llopis-Lladó, 1947; Anadón et al., 1985; Guimerà, 2004). The general structure of the CCR is essentially the result of a multiepisodic and complex Alpine evolution that included: 1) two extensional episodes from Late Paleozoic to Mesozoic, 2) a compressional period during the Paleogene, and 3) an extensional period from latest Oligocene to middle Miocene (Roca and Guimerà, 1992; Salas et al., 2001; Roca et al., 2004; Marín et al., 2008; Baqués et al., 2012).

The first extensional episode, Late Permian to Triassic in age, is related to the opening of the Neotethys. The second, latest Oxfordian to Aptian, is related to the opening of the North Central Atlantic and the Bay of Biscay (Salas and Casas, 1993; Salas et al., 2001) that later, led to the uncoupling of the Iberian Plate from the Eurasian Plate during Albian-early Santonian times (Srivastava et al., 1990; Sibuet et al., 2004).

From late Santonian, a faster opening of South Atlantic Ocean produced the northward drift of Africa and, consequently, the convergence and later collision of the recently uncoupled Iberian and Eurasian plates (Srivastava et al., 1990; Rosenbaum et al., 2002). This drastic change in the relative motion of Iberia generated the Pyrenean fold-and-thrust belt from the inversion of the Mesozoic rift-system (Muñoz, 1992; Vergés et al., 2002; Muñoz, 2017; García-Senz et al., 2019). In this scenario the contractional deformation progressed southwards leading to the inversion of the Mesozoic rift basins developed in the Iberian Plate and forming the Iberian Range and the Catalan Intraplate Chain (CIC). The preserved structure of the CIC consists of NNW-directed, ENE- to NE-trending thick-skinned and thin-skinned thrusts as well as strike-slip faults (Guimerà and Álvaro, 1990). According to preserved growth strata, the development of the CIC started during Paleocene times and progressed from northeast to southwest up to the middle Oligocene (Guimerà and Santanach, 1978; Guimerà, 1984; Anadón et al., 1985). From that moment and up to the middle Miocene, the rollback of the subduction of the Maghrebian Tethys beneath the Iberian Plate produced the extension of the eastern Iberian Plate from the development of widespread back-arc processes (Horváth and Berckhemer, 1982; Carminati et al., 1998; van Hinsbergen et al., 2014). This episode led to the formation of the northwestern Mediterranean Basin, which, in the CIC area, developed as result of the extensional reactivation of Paleogene thrusts (Roca, 2001; Gaspar-Escribano et al., 2004; Marín et al., 2008; Baqués et al., 2012). The extensionally reactivated faults were

responsible of the splitting of the CIC into a set of ENE-WSW blocks bounded by crustal-scale SE- to SSE-dipping extensional faults with kilometric displacements (Bartrina et al., 1992; Roca and Guimerà, 1992) (Fig. 1). The extension induced the development of a series of basins in the extensional fault hangingwalls filled by more than 4 km of sediments ranging in age from Oligocene to Recent (Bartrina et al., 1992) and an isostatic rebound in the footwalls up to 1.2 km (Gaspar-Escribano et al., 2004).

In this complex structural setting, the study area is located in the central part of the CCR in the transfer zone of the two major Neogene extensional faults: the Vallès-Penedès Fault and El Camp Fault (Fig. 2). This transfer zone is known as the Gaià-Montmell High, has a right-stepped *en-echelon* arrangement and is bounded southeastwards by the Baix Penedès Fault.

2.2. Stratigraphy and thickness variations

Four stratigraphic assemblages can be distinguished in the study area: the Variscan basement, the Mesozoic cover, the Paleogene fill of the Ebro Basin and Neogene basin infill of the Baix Penedès Basin (Fig. 3). From a Mesozoic stratigraphy point of view two main domains can be differentiated: the Miramar-Gaià Domain in the NW and the Montmell Domain in the SE (Figs. 2 and 3).

Paleozoic rocks of the Variscan basement have been reported and described at the bottom of the Senant-1 well in the Ebro Basin (Lanaja, 1987; Fig. 1) as well as in the adjoining Miramar Range (Julivert, 1955; Melgarejo, 1987) and Prades High (Figs. 1 and 2). The Paleozoic succession would be made up by Cambrian to Carboniferous slates with thin interbeds of Devonian carbonates (Julivert, 1955; Sáez and Anadón, 1989; Julivert and Durán, 1990) and Upper Carboniferous to Permian granitoids (Serra and Enrique, 1989; Enrique and Solé, 2004). The present work assumes similar Paleozoic rocks under the Gaià-Montmell High, which are considered as the structural basement.

Unconformably overlying the Variscan basement, the Mesozoic succession shows significant variations across the study area (Figs. 2 and 3). In the Miramar-Gaià Domain, the Mesozoic succession is thin and only includes 200 to 350 m of Triassic rocks (Fig. 3) (Virgili et al., 2006; Galán-Abellán et al., 2013; Mercedes-Martín et al., 2014). Towards the SE, however, the Mesozoic of the Montmell Domain exceeds 2 km of thickness (Salas, 1987) and is stratigraphically more complete including

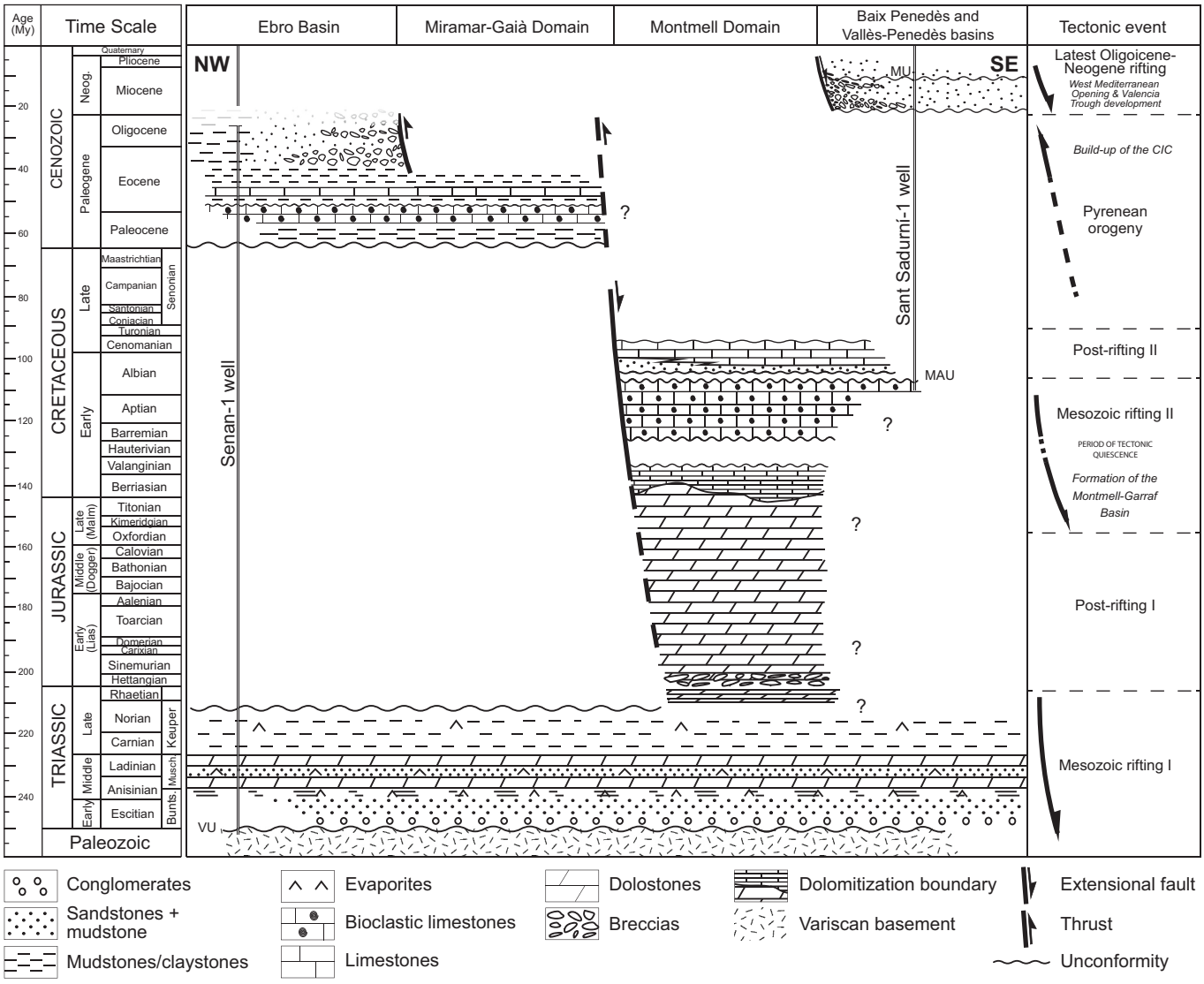

Fig. 3. Chronostratigraphic chart of the study and the adjoining areas. Main tectonic events are indicated. Major unconformities are labelled as follows. MU Messinian Unconformity; MAU: Middle Albian Unconformity; VU: Variscan Unconformity. Lithostratigraphy has been compiled from Ortí (1974), Anadón et al. (1978), Colombo (1986), Lanaja (1987), Salas (1987), Casas and Permanyer (1991), Calvet and Marzo (1994), Cabrera and Calvet (1996), Salas et al. (2001), Mercedes-Martín et al. (2014), Ortí et al. (2017) and Escudero-Mozo et al. (2017).

Triassic, Jurassic and Cretaceous rocks. On top of the Germanic Triassic, there is a 70 m-thick unit of uppermost Triassic dolomites, followed by a 300 m unit of Lower-Middle Jurassic dolomitic breccias and a 1200 m-thick succession of shallow marine limestones, dolomites and shales of Late Jurassic-Early Cretaceous age (Salas, 1987; Salas et al., 2001; Albrich et al., 2006). The Upper Jurassic-Lower Albian succession is part of a major extensional basin (the Montmell-Garraf Basin) that includes the southern end of the Vallès-Penedès Basin, the Garraf High and some adjacent offshore areas (Anadón et al., 1979; Salas, 1987; Salas and Casas, 1993) (Fig. 1). An Upper Albian to Cenomanian sequence of fluvial and shallow marine carbonates complete the Mesozoic record in the Montmell Domain (Salas, 1987; Salas et al., 2001).

Whereas Paleogene strata are absent in the Montmell Domain, the thin Mesozoic of the Miramar-Gaià Domain appears unconformably overlaid by the Paleogene sediments of the Ebro Basin infill. These are 350 to 500 m-thick marine and continental sediments, and range in age between Paleocene and early Eocene (Ferrer, 1971; Anadón, 1978; Colombo, 1986). Towards the northwest, in the undeformed Ebro Basin, the Paleogene succession thickens up to 1.5 km and includes sediments up to late Oligocene in age (Barberà et al., 2001).

Towards the E and SE of the Gaià-Montmell High, the Mesozoic succession is unconformably overlaid by the basin infill of the Vallès-Penedès and Baix Penedès basins. These sediments are made up by alluvial fan, lagoonal evaporites, carbonate coralgal and fan-delta siliciclastic deposits mainly early to late Miocene in age (Cabrera and Calvet, 1996) unconformably overlaid by Pliocene alluvial sediments (Gallart, 1981) (Figs. 2 and 3).

3. Methods

The present work is based on the construction of structural sections across the area of study using well, field data and later constrained by one 2D magnetotelluric model. Two NW-SE-oriented cross-sections have been constructed in the study area: the Gaià-Montmell section (Fig. 4) and the Marmellar section (Fig. 5). The Gaià-Montmell section is approximately 40 km long and, from NW to SE, runs from the undeformed Ebro Basin to the Baix Penedès Basin (Fig. 2). The Marmellar section is 7 km long and runs approximately 10 km east of the Gaià-Montmell section. This second section crosses the southern end of the Vallès-Penedès Fault at the NE edge of the Montmell Domain (Figs. 2 and 4). The orientations of the sections are respectively N146° and N161°, both orthogonal to the NE-SW predominant trend of the Alpine structures. The cross-sections are based on field data (mostly bedding and fault attitudes), geological map analyses and observed thicknesses of the sedimentary units. When the stratigraphic units do not crop out in the area (e.g., Lower and Middle Triassic), thicknesses have been estimated from the regional reviews of Marzo (1980) and Calvet and Marzo (1994), as well as from information from the Senant-1 and Sant Sadurní-1 wells (Lanaja, 1987, Figs. 1 and 3). The Senant-1 well has also been used to define the depth of the basement in the undeformed areas of the Ebro Basin (Fig. 3). The geometry and location of the bottom of the Baix Penedès Basin (Fig. 2) has been constrained by the gravimetric studies performed by Hernández and Casas (1985) and Casas and Permanyer (1991).

During the construction of the cross-sections, projection and extrapolation of dip data were performed defining cylindrical domains and using the kink-band method. The sections have been constructed and balanced using *2Dmove* software. To show the tectonic evolution of the area, the Gaià-Montmell section has been partially restored at the end of (a) the Mesozoic rifting phase, and (b) the contractional Paleogene deformation. During such restorations, the *line-length unfold* method (Dahlstrom, 1969), which straightens the beds while maintaining constant the line length, was used. Because the sections were constructed using the kink method, layer thicknesses remained constant during the unfolding process. This process allows calculating shortening and stretching value for each of the restored paleo-steps.

The magnetotelluric method (MT) has been used to determine the electrical properties of the upper crust across the Gaià-Montmell section and constrain the structure when possible. The MT is an electromagnetic geophysical method based on the simultaneous measurements on Earth's surface of naturally occurring electric and magnetic fields variations. The relations between electric and magnetic fields at different periods are used to define the impedance tensor whose components provide information about the electrical resistivity distribution at depth (Simpson and Bahr, 2005). This technique is very sensitive to conductive bodies that, in depth, can be associated with the presence of conductive rocks, minerals and partial melts, and also to the presence of fluids. Taking into consideration the marked lithological differences between the stratigraphic sequences present along the Gaià-Montmell section the main goals of the MT study were: 1) to recognize the geometry of the boundaries between the main stratigraphic and structural units in depth, and 2) to identify basement conductivity anomalies that could denote the presence of damage zones and fluid circulation.

4. Structure of the Gaià-Montmell High

4.1. Gaià-Montmell section

The structure of the Gaià-Montmell High is illustrated in the Gaià-Montmell section (Fig. 4). The Gaià-Montmell High relates to the positive relief located between the Baix Penedès Basin and the SE margin of the Ebro Basin, which is represented by the Carme-Cabra Anticline (Fig. 2). This anticline is an ENE-WSW-trending structure that involves the Variscan basement as well as Triassic and Paleogene sediments. It has a 13 km long and nearly horizontal backlimb and a shorter 1 km long vertical to overturned forelimb (Fig. 4 and Fig. A of the Supplementary material). This uplifted area has been interpreted as the result of the emplacement of a NW-vergent basement thrust (Gaià-El Camp Thrust), the ramp of which constantly dips less than 30° underneath the ensemble of the Gaià-Montmell High and branches at the lower part of the Montmell Fault. Such geometry is constrained by the width of the uniformly uplifted area (~13 km) and supported by the ESCI-Catalanides deep seismic profile that shows that basement-involved thrusts in the CCR do not affect the top of the lower reflective crust located at 12 to 15 km depth (Fernàndez et al., 1990; Sàbat et al., 1997; Roca et al., 2004). In this scenario, the geometry of the frontal limb of the Carme-Cabra Anticline is interpreted as controlled by a triangular zone of distributed shear at the tip of this propagating thrust (Allmendinger, 1998; Mitra and Mount, 1998; Allmendinger et al., 2004).

From a structural point of view, the Gaià-Montmell High can also be divided in two domains. In the Miramar-Gaià Domain, the hangingwall of the Gaià-El Camp Thrust is practically horizontal and shows little deformation, except for the presence of sets of minor post-Paleogene SE-directed normal faults located in the Carme-Cabra Anticline backlimb, affecting the basement and generating extensional rollovers on their hangingwalls. On the other hand, the Montmell Domain shows gentle NW-vergent fault-bend folds compatible to the presence of basement reverse faults. These and their related folds involving the basement appear affected by high-angle SE-dipping extensional faults. The syncline present east of La Juncosa, for instance, appears controlled by the emplacement of one these basement-involved faults west of Masies de Sansuies (Fig. 4). This reverse fault develops a frontal structure with a discrete, relatively steep front limb and a flat crest behind it that is similar to the overall geometry observed in the Miramar-Gaià Domain but at minor scale.

Both structural domains are separated by a highly deformed and narrow strip located SE of L'Arboçar (labeled "L'Arboçar deformation strip" in Fig. 4). In this area, Middle Triassic and Lower Ypresian (Ilerdian) rocks belonging to the Miramar-Gaià Domain are strongly deformed by NW-verging recumbent folds, thrust faults and backthrusts mostly interpreted as detached at the top of the Lower Triassic (Buntsandstein). A pre-Paleogene nearly vertical extensional basement fault

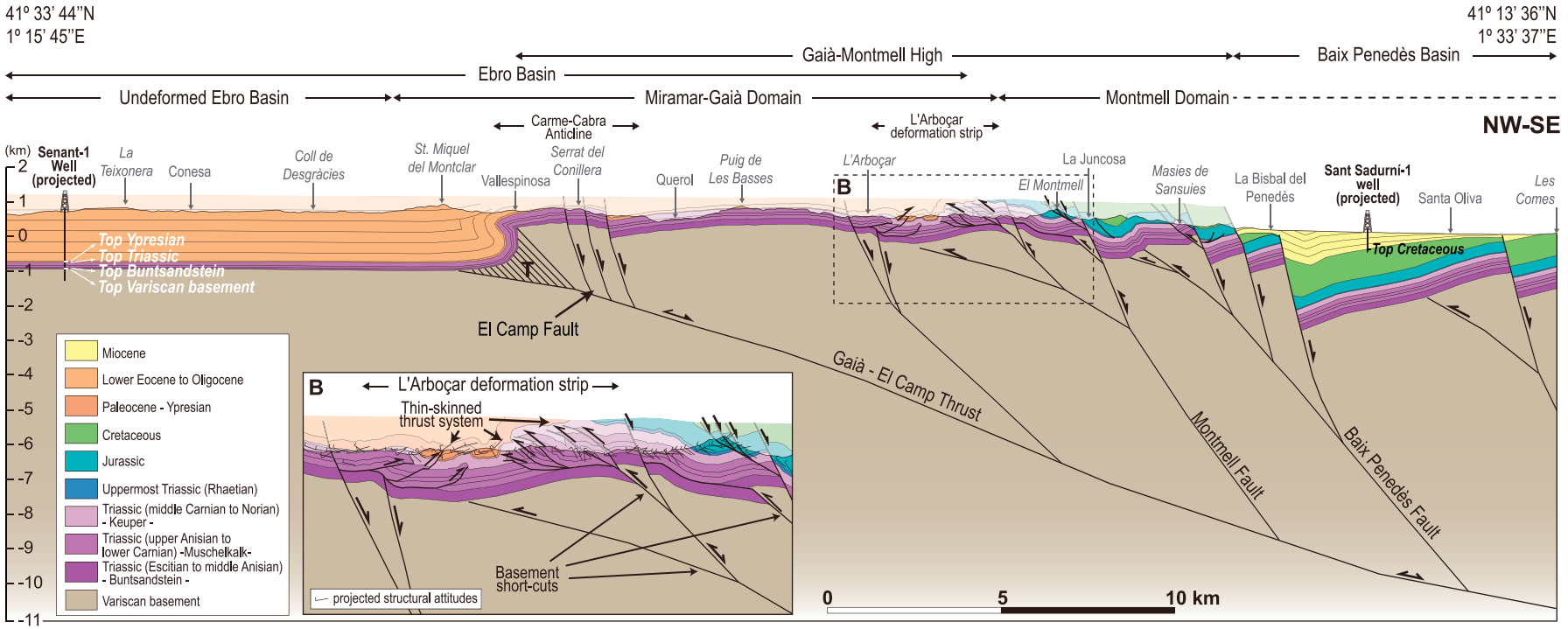

Fig. 4. Gaià-Montmell section showing the Alpine structure at the linkage zone between the Neogene Vallès-Penedès and El Camp faults in the central Catalan Coastal Ranges. See location of the section in Fig. 3. The hatched area labelled with "T" indicates the zone of distributed shear at the upper tip of the Gaià-El Camp Thrust. B) Detail of the structure of the L'Arboçar deformation strip.

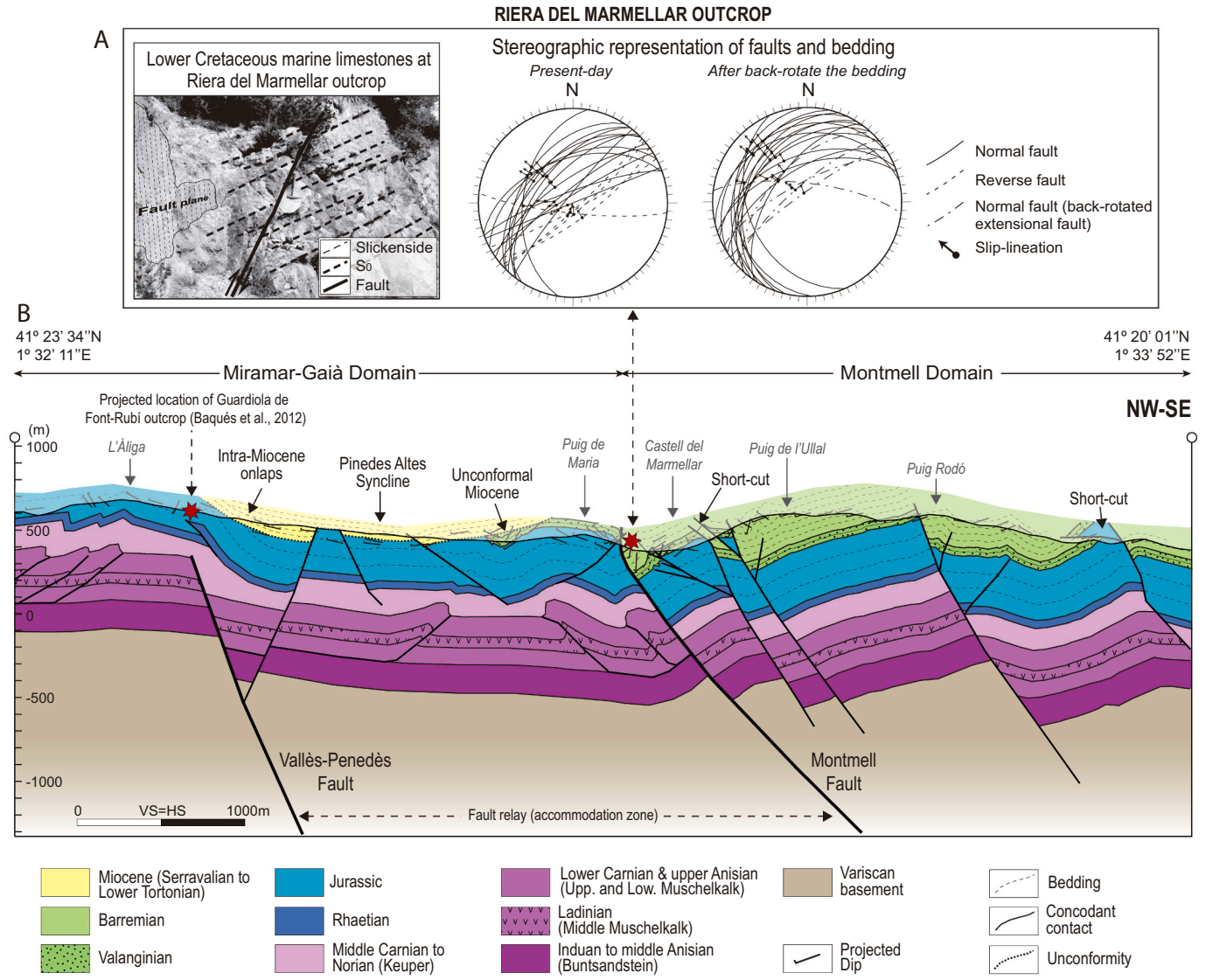

Fig. 5. A) Riera del Marmellar outcrop exemplifying collected structural data and stereographic plots (lower hemisphere) with measured fault planes and slip directions in the present-day and their orientations after unfolding the bedding. B) Marmellar Section showing the structure at the NE sector of the Montmell Domain and adjoining Miramar-Gaià Domain areas. Location of the Riera del Marmellar and Guardiola de Font-Rubí outcrops are indicated with a red star. See Fig. 3 for the location of the section and the outcrop in map view. (For interpretation of the references to color in this figure legend, the reader is referred to the web version of this article.)

seems to control the location and development of the backthrusts in the NW limit of the deformation strip. Northwest and southeast of this strip, the Triassic is located at the same structural high. However, the base of the Cenozoic occupies a significantly lower position in the Miramar-Gaià Domain than in the Montmell Domain, where the top of the outcropping thick Mesozoic succession indicates that this would be located at least 500 m higher. This structural and stratigraphic configuration, in conjunction with the NW vergence of the structures developed along the L'Arboçar deformation strip, suggest interpreting the NW limit of the Montmell Domain as a nearly complete inverted SE-dipping Mesozoic extensional fault. In this scenario, the L'Arboçar deformation strip would correspond to the transmission of the compressional deformation to the Montmell Fault footwall, which induced the formation of detachment folds and thin-skinned thrusting facilitated by the presence of evaporitic decollement levels within the Triassic (Fig. 4).

The age of this suggested inversion of the Montmell Fault is poorly constrained due to the lack of preserved growth and post-growth strata around this fault. Only the presence of Paleocene to lower Ypresian strata contractionally deformed in the L'Arboçar deformation strip indicates that it had to take place after early Ypresian (post-Ilerdian). On the other hand, the development of the Gaià-El Camp thrust sheet is well constrained by the presence of syntectonic sediments preserved in the Sant Miquel del Montclar area (Figs. 2 and 4). At this location, the Carme-Cabra Anticline forelimb presents series of NW-dipping upper Eocene conglomerates unconformably overlying overturned lower Eocene conglomerates, sandstones and mudstones (Anadón et al., 1985). These growth geometries allow establishing the age of the emplacement of the Gaià-El Camp thrust sheet as middle Eocene.

The Gaià-Montmell section also shows several extensional faults affecting the previously outlined compressional structure. A set of SE-dipping, basement-involved extensional faults bound the Baix Penedès Basin towards the NW and show an accumulative displacement of about 2.5 km. The existence of the Mesozoic succession underneath the Baix Penedès Basin remains uncertain due to the absence of subsurface data in this area. However, we assume its presence taking into consideration data from the Sant Sadurní-1 well, which cuts fossil-rich limestones rocks of Early Cretaceous age (Neocomian) (Lanaja, 1987; see Fig. 1 for its location).

In addition, a set of minor SE-dipping faults that affect Mesozoic and Paleogene strata of the Carme-Cabra Anticline backlimb is present between the villages of Vallespinosa and Querol as well as NW of L'Arboçar. Cartographically, these faults are NE-SW-oriented, laterally disappearing towards the NE (Fig. 2), they display relatively high angles (>75°) and show metric to decametric fault throws. Taking into consideration roll-over geometries and the fact that they are only present in the Gaià-El Camp thrust sheet hangingwall, these are interpreted as rooted in the Gaià-El Camp Thrust. If this fault linkage exists, this would imply the Gaià-El Camp Thrust plane also underwent extensional reactivation during the Neogene.

4.2. Marmellar section

The Marmellar section is located at the southeast of the Gaià-Montmell High and includes the southeasternmost part of the Miramar-Gaià Domain, the SW end of the Vallès-Penedès Fault and the Montmell Domain (Figs. 2 and 5). At this location, the Miramar-Gaià and the Montmell domains are separated by a NE-SW-oriented fault that laterally corresponds to what has been described in the Gaià-Montmell section as the Montmell Fault. Additionally, the section is adjacent to the Mesozoic succession-type described by Salas (1987) and labeled "M" in Fig. 2, which allows a detailed recognition of the Mesozoic rocks outcropping in the area.

The structure of the Montmell Domain belongs to an array of NE-SW-oriented, SE-dipping basement extensional faults that split the area into a system of NW-tilted fault blocks filled by up to 1100 m thick Jurassic to Barremian rocks (Fig. 5). These faults have throws of hectometric displacement up to 300–400 m and kilometric lengths up to 5 km, which allows considering these extensional faults as vertically restricted (Nicol et al., 1996). At depth, these basement-involved extensional faults show domino style dipping 55–60° towards the SE and display reverse and normal drag folding in their hangingwalls. Moreover, minor compressional features deforming the Mesozoic sedimentary cover are present the Montmell Domain. Basically, these are represented by SE-directed reverse faults and low angle NE-vergent thrusts respectively located at the hangingwalls and footwalls of some of the major extensional faults.

Structural data was collected at the Riera del Marmellar outcrop in Lower Cretaceous marine limestones belonging to the Montmell Fault hangingwall. At this location, beds are 1 to 4 m-thick, trend NE-SW, dip around 31° to the NW and contains metric-scale faults, tension veins and numerous stylolite surfaces. Gathered structural data mainly consists of normal faults with orientations ranging N30–70, dipping 65 to 80° towards the NW with 80°WNW of slip, as well as reverse faults with orientations N50–65, dipping 70 to 80° towards the SE with 70°E of slip. Data was displayed on stereoplots and later restored to their original geometry by rotating bedding to horizontal (Fig. 5). Once restored, all collected faults originally look as normal faults with orientations mainly ranging N15–75, dipping 30 to 85° towards the NW and with slip direction towards the NW. Fluid geochemistry analysis performed by Baqués et al. (2012) in the same area relates these mesostructures to the Mesozoic *syn*-rift stage that led to the development of the Montmell-Garraf Basin.

The Montmell Fault, a basement-involved SE-dipping extensional fault, represents the NW boundary of the Montmell Domain. This fault is nearly vertical (>85°) at surface that progressively decreases its dip at depth up to 45°. This major structure also coincides with the NW boundary relatively thick Lower Cretaceous successions outcropping in the Montmell Domain, the map view configuration of which corresponds to series of NE-SW-oriented normal faults separated by narrow transfer zones that can be correlated with the presence of a basement fault that becomes segmented at surface (Fig. 2). Its interpreted location matches the NE prolongation of the Montmell Fault as interpreted in the Gaià-Montmell section (Fig. 4). Contractional structures such as low-angle NW-directed thrusts and their related fault-bend and fault-propagation folds are present in the Montmell Fault footwall. These structures involve Jurassic and Middle to Upper Triassic rocks and, because of they show short wavelengths in the geological map, they have been interpreted as rooted at the evaporitic levels of the uppermost Lower Triassic (Buntsandstein) that is considered a good regional detachment.

At surface, the Miramar-Gaià Domain is characterized by a Jurassic to Miocene cover deformed in a 2 km-wide gentle syncline (Pinedes Altes Syncline, Fig. 5) bounded towards the NW by a SE-dipping monocline. Miocene is only present in this syncline and unconformably overlies Lower Cretaceous and Jurassic rocks that show a more thigh syncline geometry. The syncline appears affected by some minor extensional faults mainly developed at its lower part and includes internal onlaps in its NW limb. At smaller scale, the outcropping Jurassic-Lower Cretaceous cover appears affected by minor NW and SE-verging folds. These, locally cut by small thrusts, are interpreted as drape/fault-bend folds developed over Muschelkalk thrust horses limited by the Keuper and the uppermost Buntsandstein evaporite decollements.

The NE-SW orientation of the monocline limiting the Pinedes Altes Syncline to the NW and its lateral continuity with the cartographic trace of the Vallès-Penedès Fault towards the NE allow interpreting this structure in the Marmellar section. In map view, the Vallès-Penedès Fault shows splays and relay faults developed at the termination of a fault segment. Approximately 1 km NE of the Marmellar section, Jurassic rocks outcrop in both the hangingwall and the footwall of the Vallès-Penedès Fault denoting the loss of displacement of this towards the SW (Fig. 2). Therefore, in the Marmellar section, the Vallès-Penedès Fault has been interpreted as a SE-dipping (~65°) basement-involved normal fault that dies out in the Upper Triassic interval and drape folds the overlying Jurassic and Miocene rocks.

Based on these geometrical relationships, it is possible to establish the relative kinematic ages of some of the structures illustrated in the Marmellar section. The relatively thick Mesozoic succession and the structural data collected in the Riera del Marmellar outcrop (Fig. 5), indicate this fault experienced extensional motion during, at least, the Lower Cretaceous coevally to the formation of the Montmell-Garraf Basin (Salas, 1987). Compressional features along the Montmell Fault cartographic trace are essentially located in its hangingwall and affect Mesozoic rocks. This may suggest a post-Lower Cretaceous compressional phase that, at this location, did not reactivate the Montmell Fault but developed buttressing against the previously formed extensional fault (Gillcrist et al., 1987; Cooper et al., 1989). Minor reverse faults also developed in the Miramar-Gaià Domain, basically consisting of NW- and SE-directed thrusts at the NW and SE limbs of the Pinedes Altes Syncline and affecting Jurassic rocks (Fig. 5). Although the age of the compression is poorly constrained by preserved strata (mostly Mesozoic rocks coeval or previous to the extensional phase), it is possible to sustain that compression occurred after their deposition (post- Lower Cretaceous), and previously to the deposition of the Miocene sediments that unconformably overlie the observed contractional structures. This fact makes possible relating the compressional features observed in the Marmellar area to the regional compressional phase that affected the central part of the CCR during Paleocene to Eocene. On the other hand, onlap geometries in Miocene sediments preserved above the monocline that characterizes the NW limb of the Pinedes Altes Syncline indicate these sedimented deposited during the extensional motion of the Vallès-Penedès Fault during Miocene times.

5. Magnetotelluric data and 2D inversion model

Nineteen magnetotelluric (MT) soundings with recording times ranging from 8 to 12 h were acquired along the Gaià-Montmell section (Fig. 2). Time series were processed using the Egbert and Booker (1986) method and applying remote reference when possible. Apparent resistivity and phase resulting curves cover periods from 0.001 s to 1 s.

To determine if the geoelectrical structure is 1D, 2D, 3D/2D (2D structures with galvanic distortion) or 3D, a dimensionality analysis was performed using the WALDIM code (Martí et al., 2009b) that is based on

the invariant rotation parameters of the impedance tensor. The dimensionality results (Fig. B of the supplementary material) show that for periods shorter than 1 s, this behavior can be considered highly variable with a rather frequent 2D component, whereas at periods longer than 1 s, the geoelectrical behavior is strongly 3D. In all 2D and 2D/3D cases, the strike is rather parallel with a trend that ranges between N015° and N065°; orientation that is consistent with the N40–60° trend of the geological structures (Figs. 1 and 3). So, the dimensionality analysis results reveal that a 2D MT model could be rather reliable to determine the geoelectrical structure in periods shorter than 1 s, but not at longer ones where the dominant 3D data structure can induce wrong interpretations (Ledo, 2005). Considering this dimensional breakdown, a directionality analysis was performed using the STRIKE code developed by McNeice and Jones (2001). It states a geoelectrical direction of N55° although it also indicates a 3D effect of the regional structure. The elements of the impedance tensor were rotated applying this direction to obtain the two main directions for the 2D modeling: the transverse electric (TE) mode when the electric field is parallel to the strike and the transverse magnetic (TM) mode if the parallel one is the magnetic field. The obtained apparent resistivity and phase curves for each sounding are shown in the Fig. C of the Supplementary material. Data and model responses are presented as pseudo-sections built by plotting the data in an x-T map, where x-axis corresponds to the data position on the profile and T-axis to the period, which is considered as a proxy of the depth: TE and TM apparent resistivity and phase responses (Fig. D of the Supplementary material).

The 2D modeling is based on the simultaneous fit of the TE and TM data and has been done using the 2D RLM2DI inversion code (Rodi and Mackie, 2001) considering a 5% error floor that reaches an RMS of 2.7. The final 2D model is presented in Fig. 6A, which shows the calculated apparent resistivities.

5.1. Correspondence between the 2D magnetotelluric model and the Gaià-Montmell section

The MT model illustrates the geoelectrical structure along the Gaià-Montmell section with the presence of different conductivity/resistivity bodies (Fig. 6A). In general terms, the MT model shows a geoelectrical structure shaped by two stacked up layers. The lower layer has a very resistive (≥1000 Ω·m) and homogeneous character below 0.5–2.5 km, although some less-resistant bands (~100–600 Ω·m) are also present (e.g. below the Montmell Domain and the NW limit of the Miramar- Gaià Domain). The geoelectrical behavior of the upper layer is, on the other hand, highly heterogeneous where the presence of conductive bodies with low lateral continuity (mostly isolated conductive bodies) prevails.

The comparison between the resistivity model and the Gaià-Montmell section (Fig. 6B) allows the correlation of the geoelectrical structure to different types of rheologies. The highly resistive and laterally continuous response of the lower geoelectrical layer (R1 and R3, Fig. 6A) can be correlated to the Variscan basement, which is made up by epimetamorphic and plutonic rocks. The high resistivity of the basement is corroborated by two additional parametric MT soundings acquired 30 km southwest of the study area in the Prades High on top of Paleozoic rocks (soundings Pz1 and Pz2, see Fig. 1 for location). MT soundings at this location reveal that Carboniferous slates and Permian granitoids show resistivities ≥1000 Ω·m (Fig. E in the supplementary material), fact which is also documented in other locations of the Iberian Peninsula such as the Iberian Massif (Muñoz et al., 2008), the Pyrenees (Ledo et al., 1998; Campanyà et al., 2018) and the Betic Cordillera (Martí et al., 2009a; Rubinat et al., 2010).

The upper geoelectrical layer is, instead, very variable in depth and in resistivity character. From NW to SE, it includes conductive/resistive bodies C1, C2, C3, C4, R2, C5 and C6. Comparing the geoelectrical character to geological data and interpretations along the Gaià-Montmell section (Fig. 6B), these bodies can be divided in two different groups, those that correlate with the Mesozoic and/or Cenozoic sedimentary cover (C1, C2, R2, C5 and C6) and those that suit with positions of the Variscan basement (C3 and C4). Located in the northernmost part of the section, C1 agrees with the Mesozoic and Cenozoic sedimentary infill of the Ebro Basin, the thickness of which accounts to 1649 m of sedimentary cover above the Variscan basement as described in the Senan-1 well (Lanaja, 1987; see Figs. 1 and 3 for well location).

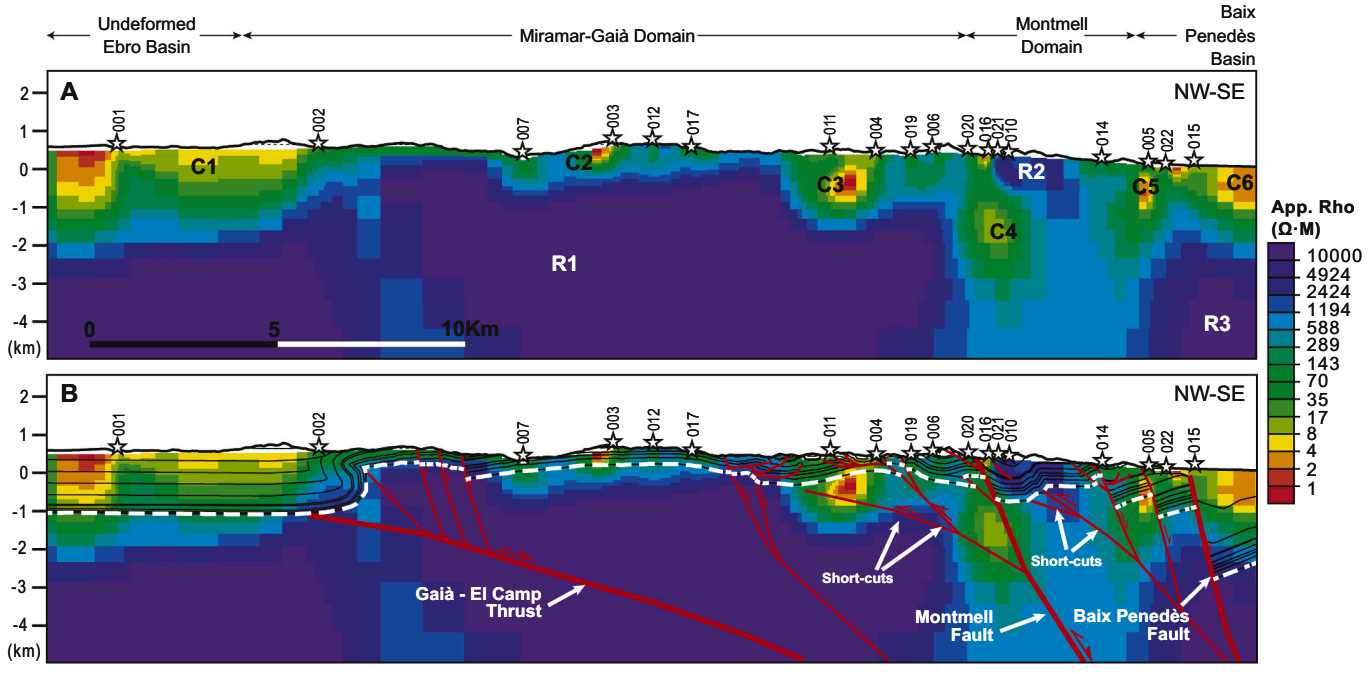

Fig. 6. A) Final magnetotelluric 2D model of the Gaià-Montmell section showing the differentiated conductive (C labels) and resistive (R labels) bodies. B) The model with the interpreted stratigraphic boundaries (black lines), faults (red lines) and the top of the Variscan basement (dashed white line). White stars indicate the location of the MT soundings (see Fig. 3 for their location). (For interpretation of the references to color in this figure legend, the reader is referred to the web version of this article.)

Likewise, conductive body C2 coincides in thickness and location with the Triassic succession, which, in the Miramar-Gaià Domain, mainly consists of clastic sediments with evaporitic episodes and carbonates (Fig. 3). On the other hand, resistive body R2 agrees with the position of Jurassic and Lower Cretaceous rocks, which mainly consist of massive limestones and dolostones present in the Montmell Domain. Geoelectrical body C5 also coincides with the clastic sediments with evaporitic and carbonate episodes of the Triassic of the southeastern Montmell Domain. At the southeastern end of the section, the conductive body C6 agrees with the Neogene infill of the Baix Penedès Basin, the thickness of which is pointed out by Casas and Permanyer (1991) as approximately 2000 m of mainly terrigenous sediments (Cabrera and Calvet, 1996).

Taking into consideration the intrinsic resistive character of the Variscan basement, the explanation about the nature of the conductive body C3 is conjectural. Low resistive values at this location ($\leq$10 Ω·m) can be related to highly fractured rocks (e.g., Pous et al., 2001; Martí et al., 2020) and/or metallic mineralizations (Martí et al., 2009a) similar to those recognized in the central CCR southwest of the study area in the Prades High (Fig. 1). Examples of documented metal mineralizations in this area consist of Pb-Zn-Ba-Ag-Ni-Cu sediment-hosted veins, late Hercynian to Triassic in age, formed along intra-Paleozoic and Lower Triassic fractures (Cardellach et al., 1990; Canet et al., 2005; Alfonso et al., 2012). Hence, metal mineralizations, which include highly conductive elements, would enhance the conductive character of the Variscan basement rocks at C3 (Fig. 6).

The geoelectrical body C4 belongs to a 1–2 km wide, SE-dipping band of relatively low resistivity ($\geq$15 Ω·m) 2 km depth underneath the NW limit of the Montmell Domain (Fig. 6). This band is clearly differentiated from the surrounding high resistive and homogeneous signature that characterizes Variscan basement and appears in agreement with the location of the NW limit of the Montmell Domain. The origin of this low resistivity is uncertain, although it seems to be related to a different type or degree of deformation between the Miramar-Gaià and the Montmell domains. While the Miramar-Gaià Domain formed during the Paleogene compression concentrating its deformation at the tip of the Gaia-El Camp Thrust and the frontal limb of the Cabra-Carme Anticline, the structural analysis in the Montmell Domain indicates a higher degree of deformation that includes thick-skinned extensional and contractional structures. The Variscan basement is highly deformed in the central CCR and only planar-type Paleozoic structures such as low-angle thrusts have been described (Julivert and Durán, 1990). However, this type of geometries does not suit with the description of C4. Considering C4 is related to the presence of a SE-dipping basement fault, its 1 to 2 km width would correspond to the damage zone located at the Montmell Fault footwall where conductivity has been enhanced by the presence of fluids within a fractured and permeable zone (e.g., Pous et al., 2001) and, perhaps, metal conductive mineralizations.

Considering these interpretations, the MT model has allowed constraining three key structural aspects along the Gaià-Montmell section (Fig. 6): 1) the depth of the base of the Mesozoic to Cenozoic sedimentary infill of the Ebro Basin over the Variscan basement in the northernmost sector (conductive body C1 between MT soundings 001 and 002); 2) the geometry of the Montmell Fault underneath the northern limit of the Montmell Domain and the location at depth of its related shortcut (conductive body C4 between MT soundings 020 and 010); and 3) the base of the Mesozoic to Miocene sedimentary infill of the Baix Penedès Basin in the southernmost sector (conductive body C6 south of the MT sounding 015).

6. Discussion: tectonic evolution and structural inheritance of the central CCR

Structural and stratigraphic observations along the Gaià-Montmell and Marmellar sections, together with regional geophysical data and geological maps allow the characterization of the deformation history of the linking zone between the Vallès-Penedès and El Camp basins (Figs. 1 and 2). The tectonic evolution of this area includes three major Alpine events: A Late Jurassic-Early Cretaceous extension, a latest Cretaceous-early Oligocene compression and uplift, and a late Oligocene-Neogene extension.

6.1. Late Jurassic (Oxfordian) – early cretaceous extension: Montmell-Garraf Basin formation

The Alpine cycle regionally starts with a Late Permian-Early Triassic extensional period that controlled the deposition of siliciclastic and carbonate units along NE-SW-trending basins (Galán-Abellán et al., 2013; Mercedes-Martín et al., 2014; Mercedes-Martín and Buatois, 2020). However, in the study area Triassic strata show no lateral thickness variations indicating a relative tectonic quiescence during this period. The first hints of Mesozoic tectonic activity do not appear until the Late Jurassic. Upper Oxfordian to Valanginian carbonate-dominated sediments deposited in an incipient depocenter (the Montmell-Garraf Basin), bounded towards the NW by a high-angle SE-dipping extensional fault. The constant thickness of the Valanginian sediments indicates they were deposited over a planar extensional ramp (McClay, 1995; Withjack and Schlische, 2006; Ferrer et al., 2016). This fault would correspond to the breakaway fault of the extensional system, the present-day location of which corresponds to the SE limit of L'Arboçar deformation strip (Fig. 4). Laterally towards the NE, this fault corresponds to the SW prolongation of the Vallès-Penedès Fault (Figs. 2 and 5).

Late Valanginian to Hauterivian strata are absent in the Montmell-Garraf Basin and Barremian sediments paraconformably overlie preserved Valanginian (Fig. 5). This hiatus throughout the Neocomian is widespread recognized in the region and, with a diachronic character, has been interpreted in two ways: as a period of decelerated subsidence, emersion and relative tectonic quiescence in the external zones of the rift basin system (Anadón et al., 1979; Salas et al., 2001), or related to a thermal post-Late Jurassic-early Valanginian rifting phase (Salas et al., 2020). From Barremian on, an acceleration of the subsidence takes place in the Montmell-Garraf Basin following two different phases: 1) Barremian to early Albian, 2) late Albian to Cenomanian. During this period, the breakaway fault shifts towards the SE to the present-day location of the Montmell Fault (Figs. 4 and 5). Considering this scenario, the Montmell Fault, can therefore be considered as the SW segment of a major structure that we call the Montmell-Vallès Fault System.

Barremian to Lower Albian sediments were deposited in the Montmell-Marmellar area with significant thickness variations. Up to 550 m of Barremian to Lower Aptian shallow marine carbonates deposited on the Montmell Fault hangingwall in the Marmellar area. In comparison, towards the NW in the Miramar-Gaia Domain, Paleocene sediments conformably lie over Triassic strata (Fig. 4) and Jurassic to Cretaceous sediments are absent. This fact can be explained by erosion or non-deposition. The nonexistence of clastic deposits during this period, which would represent the erosion of Jurassic and Cretaceous strata before the Paleocene, most likely indicates a hiatus scenario due to the presence of a paleo-structural high NW of the Montmell Fault (Ebro High, Fig. 7C) during, at least, the extensional motion of the Montmell Fault from Barremian to early Albian.

The end of the extensional motion of the Montmell Fault cannot be established with precision with the analyzed data. However, regional criteria associate the end of the extension to the development of the Middle Albian Unconformity (Fig. 3) (Salas, 1987; Salas et al., 2001; Salas et al., 2020). From this time and up to the Cenomanian, a relatively constant thickness unit characterized by the entrance of clastic sediments is deposited (Salas and Casas, 1993). This period has been traditionally interpreted as post-rift thermal relaxation with associated homogeneous subsidence (Robles, 1982; Alonso et al., 1993; Salas et al., 2001). However, new interpretations relate this period to late crustal extension over a low angle fault that passively transports the area

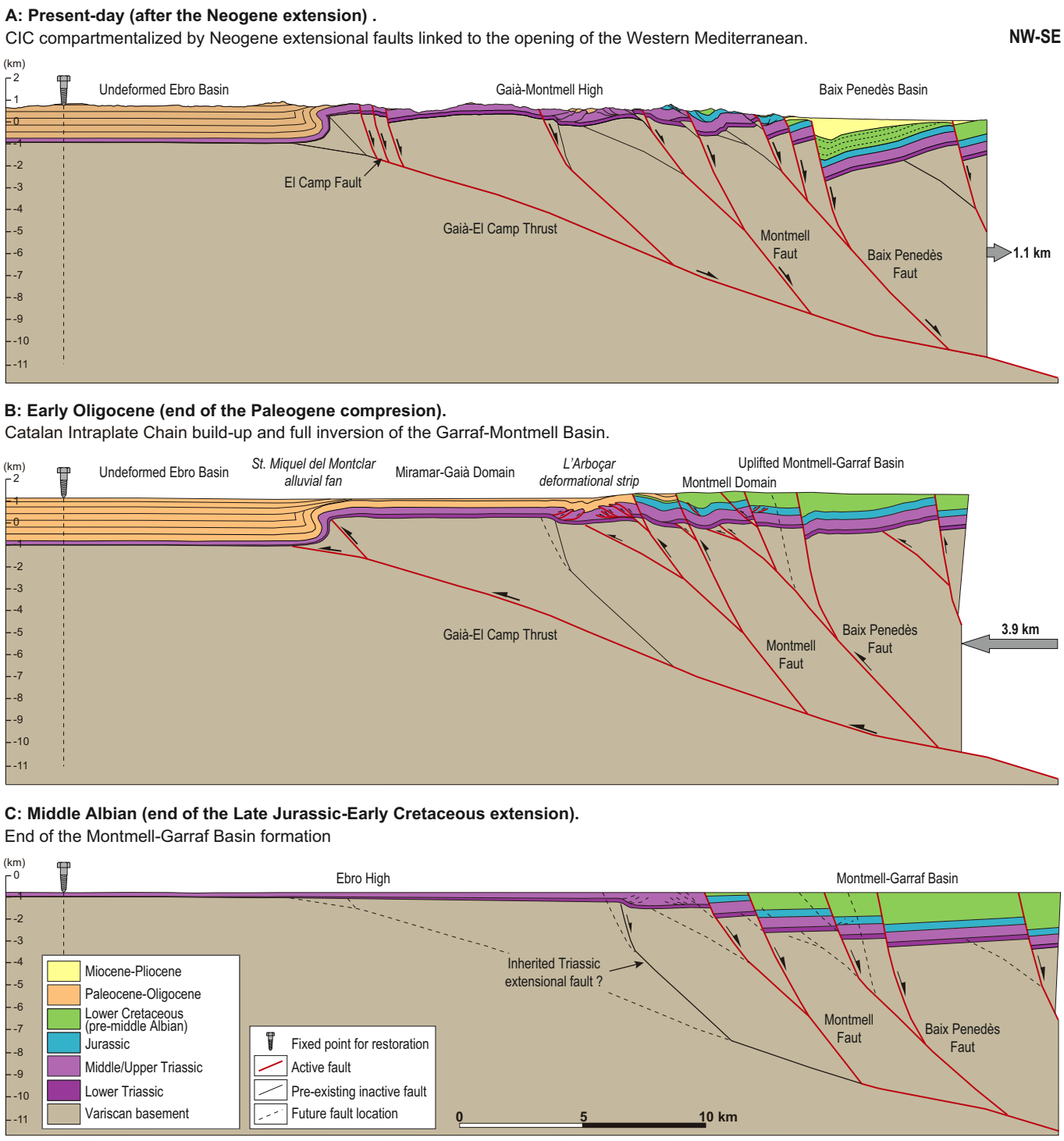

Fig. 7. Sequential structural restoration of the Gaià-Montmell section applying flexural slip and bed lenght preservation. A) Present-day after the latest Oligocene-Neogene extension. B) Early Oligocene (end of the Paleogene compression). C) Late Cenomanian (end of the Late Jurassic-Early Cretaceous extension). No vertical exaggeration.

previously formed by high-angle extensional faults (Tugend et al., 2015) and, hence, with the resulting extensional displacement of the Montmell Fault.

6.2. *Late cretaceous - early Oligocene compression: positive inversion of the Montmell Fault and emplacement of the Gaià-El Camp thrust sheet*

From late Santonian (Late Cretaceous), the convergent motion between the Iberian and Eurasian plates is activated (Roest and Srivastava, 1991; Rosenbaum et al., 2002), yet the transmission of compressional stresses into the study area arises in the lattermost Cretaceous (Maastrichtian?). During this period of the convergence, up to three phases can be distinguished. The first phase takes place at the end of the Cretaceous and is recorded in the Miramar-Gaià Domain by the presence of a paraconformity that brings the basal Paleocene and the Keuper into contact (Figs. 3 and 4). The presence of this unconformity indicates a regional pre-Paleocene uplift that can be linked to an uppermost Cretaceous contractional deformation over the entire area or, conversely, to an

isostatic adjustment of the Montmell Fault footwall after the Late Jurassic to Lower Cretaceous rifting phase. From a tectonic point of view, this period can be both contractional and quiescent. The second phase occurs from Paleocene to early Eocene times, and is characterized by the sedimentation of concordant fine-grained terrigenous beds and carbonates with little lateral thickness variations deposited in the distal areas of the Pyrenean foreland (Anadón et al., 1979; Anadón et al., 1985). These deposits indicate the absence of significant deformation or creation of relief in the adjacent areas of the central CCR and, therefore, a period of tectonic quiescence. The third and most relevant compressional phase in the study area takes place from Middle Eocene to early Oligocene. During this period compressional structures emerged in both Miramar-Gaià and Montmell domains. The footwall of the Montmell Fault was strongly deformed by a set of basement shortcuts that laterally become thin-skinned-controlled fold-and-thrust systems detached at top Buntsandstein and Keuper evaporitic levels. On the other hand, minor deformation appeared in the Montmell Domain where SE-vergent backthrusts and pop-up structures developed (Figs. 4 and 5), possibly as a result of slight buttressing effect. This structural style around the Montmell Fault is also observed in several parallel minor extensional faults in the Montmell Domain (Figs. 4 and 5), which denote the contractional reactivation of pre-existent Mesozoic extensional faults in the area. The tectonic inversion is basically characterized by minor hangingwall buttressing later passively transported by shortcuts developed in the upper part of the reactivated faults, and thin-skinned thrust systems detached in the Triassic evaporite levels of the Miramar-Gaià Domain.

The whole ensemble of the Miramar-Gaià Domain became uniformly uplifted by the Gaià-El Camp Thrust. Considering the dip of this thrust and the fact that it merges at depth to the Montmell Fault, the Gaià-El Camp Thrust can be interpreted as a major footwall shortcut developed to provide a smoother fault trajectory during the inversion of the Montmell Fault (Fig. 7B).

Paleogene growth geometries at the SE margin of the Ebro Basin consisting of Upper Eocene to lower Oligocene sediments unconformably deposited over Lower to Middle Eocene strata (St. Miquel del Montclar area, Figs. 4 and 7B) allow establishing the precise age of the Gaià-El Camp Thrust emplacement as late Bartonian to Lower Oligocene. Conversely, the age of the inversion of the Montmell-Garraf Basin cannot be fully constrained due to the lack of preservation of growth sequences. Nevertheless, taking into consideration that up to Lower Ypresian (Ilerdian) sediments are involved in the Montmell Fault footwall deformation with no growth geometries, it can be stated that the contractional motion in this area is, at least, late Ypresian (Cuisian). Additionally, the fact that the Gaià-El Camp Thrust has been interpreted as a major shortcut supports the idea that the primary reactivation of the Montmell Fault was to some extent older (late Ypresian to Lutetian).

6.3. *Latest Oligocene(?)/early Miocene - late Miocene extension: Baix Penedès Basin formation and partial reactivation of the Gaià-El Camp Thrust*

The Paleogene structure described in the previous section is affected by extensional deformation that cuts or, at times, reactivates previously formed faults. Most of the interpreted extensional faults have a predominant ENE-WSW orientation, dip towards the SE and generally display decametric to hectometric displacements (Figs. 2 and 7A). Four major faults (Vallès-Penedès, Montmell, El Camp and Baix Penedès faults) show kilometric fault traces and display an overlapped arrangement linked by large NW-SE-oriented accommodation zones (Fig. 8).

The Vallès-Penedès Fault progressively loses its displacement towards the SW overstepping with the Montmell and the Baix Penedès faults in the respectively Marmellar and Sant Martí Sarroca transfer zones (Fig. 8). In this area, the Vallès-Penedès Fault throw becomes less than 300–400 m, displaying a drape-fold detached in the Upper Triassic evaporites on its hangingwall (Fig. 5). Extensional displacement is,

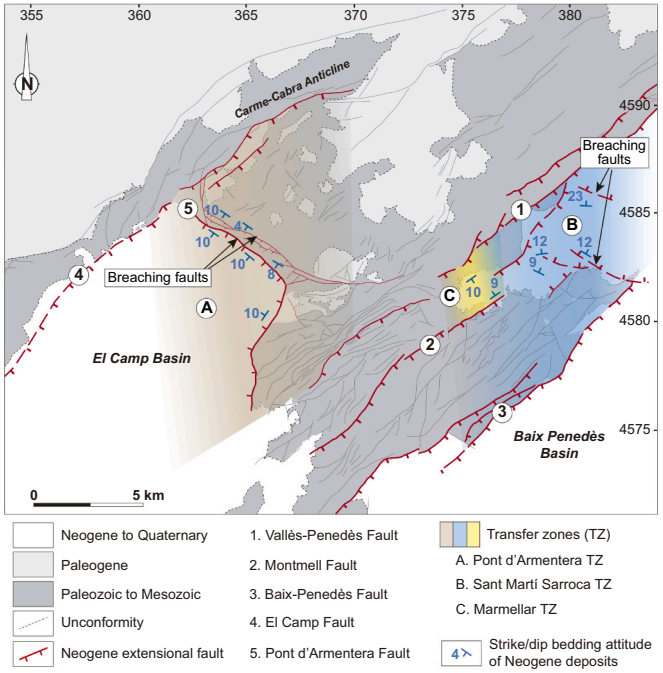

Fig. 8. Schematic geological map of the Gaià-Montmell High showing the major Neogene extensional faults and their related relay ramps.

hence, relayed to the Montmell and the Baix Penedès faults, which extends towards the SW with a similar orientation. The Montmell Fault shows decametric fault throws and a low accumulated extensional displacement. The Baix Penedès Fault, in turn, shows a segmented fault pattern with several SE-dipping splays at surface and a considerably higher accumulated throw reaching several hundreds of meters. NW-SE-trending breaching faults are present in the Sant Martí Sarroca Transfer Zone (Fig. 8). The Baix Penedès Fault is interpreted as rooted at the deep NW-vergent basement ramp underneath the area (Fig. 7).

On the other hand, the displacement of the El Camp Fault drastically decreases towards the NE and becomes a narrow array of SE-dipping faults with hectometric accumulated displacements at the Carme-Cabra Anticline backlimb (Figs. 2 and 8). Considering the geometry of the Miramar-Gaià Domain as the result of the displacement and uplift over a low angle basement ramp shallowing towards the NW (Fig. 7B), this array of extensional faults at the NE end of El Camp Fault has been interpreted as rooted in the Gaià-El Camp Thrust (Figs. 4 and 7A).

In this context of overlapped major extensional faults, the NW-SE-trending faults present in the Sant Martí Sarroca Transfer Zone as well as the Pont d'Armentera Fault (Fig. 8) are considered as relay ramp-breaching faults of a soft linked extensional system (Fossen and Rotevatn, 2016). These zones would transfer displacement between the Vallès-Penedès and the Baix Penedès faults and between El Camp Fault and the Montmell-Vallès Fault System respectively.

The extensional reactivation (or negative inversion) of preexisting faults is suggested by several evidences such as: 1) the development of an array of extensional faults rooted at the discrete fault plane of the Paleogene Gaià-El Camp Thrust at the NE end of El Camp Fault; 2) the extensional geometry of the Montmell Fault (although this fault has a reverse movement during Paleogene times); or 3) the Baix Penedès Fault and its splays which are also rooted at a Paleogene reverse fault footwall ramp. However, the reactivation of the Montmell Fault is relatively limited, and the extension seems basically relayed to the Baix Penedès Fault, which induced the development of a 1.5 km deep basin on its hangingwall (Fig. 7A).

All these structural observations indicate a post-early Oligocene extensional period that resulted in the extensional reactivation of the previously formed Paleogene and Late Jurassic-Early Cretaceous faults,

the age of which can be constrained based on the tectonostratigraphic relationships. Undeformed Pleistocene alluvial deposits fossilize most of the major faults in the central CCR, hence, indicating their extensional motion is pre-Pleistocene. Additionally, major faults, which often show drape-folds on their hangingwalls, cut or fold Serravallian sediments. Therefore, their extensional motion must be considered as post-Serravallian. Yet, extensional growth strata geometries are indeed observed in upper Serravallian-lower Tortonian sediments deposited over the hangingwall of the Vallès-Penedès Fault in the Marmellar area (Fig. 5), which would indicate, at least for this fault, extensional motion during this period. This fact agrees to previous regional studies that indicate extension in the CCR occurred between Burdigalian and Messinian times (Gallart, 1981; Cabrera et al., 1991; Cabrera and Calvet, 1996; Porta and Civís, 1996; Cabrera et al., 2004). The lack of upper Oligocene and Neogene sediments preserved over in the Miramar-Gaià and Montmell domains prevent establishing a relative chronology of the observed extensional faults.

7. Conclusions

A new field-based dataset integrated with MT data acquired across the Gaià-Montmell High has allowed the recognition of the main features characterizing the upper crustal Alpine structure. MT data along the Gaià-Montmell section has allowed a better definition of the structure at depth and the identification of zones with potential fractures and conductive fluids.

The structure of the Gaià-Montmell High consists of two domains with a differentiated tectono-stratigraphic evolution: the Miramar-Gaià and the Montmell domains. The Miramar-Gaià Domain belongs to an area with a very thin Mesozoic succession (only Triassic) uplifted over the Ebro Basin by a NW-vergent low-angle basement thrust (the Gaià-El Camp Thrust). The Montmell Domain belongs to an area with a well-developed Mesozoic succession that includes Triassic, Jurassic and Cretaceous rocks. This domain is limited towards the NW by the Montmell Fault and its structure consists of NW-vergent compressional faults affected by high-angle SE-dipping extensional basement faults. A highly deformed area with prominent NW-vergent thrust imbrications characterizes the limit between the two domains.

The Montmell Fault corresponds to the SW prolongation of the Vallès-Penedès Fault. Both faults are partially overlapped and linked by the Marmellar Accommodation Zone. We call this major structure the Montmell-Vallès Fault System. This constituted the NW limit of the Montmell-Garraf extensional basin, which developed during the Late Jurassic-Early Cretaceous (Oxfordian to middle Aptian).

A period of tectonic inversion and contractional reactivation related to the Paleogene compressional phase is attested by the presence of highly deformed areas (thin-skinned thrusting and footwall shortcut development) along the Montmell-Vallès Fault System footwall. These contractional structures belong to the positive inversion of the Mesozoic Montmell-Garraf Basin and the emplacement of a NW-directed basement thrust (Gaià-El Camp Thrust) that uplifted the Montmell-Garraf Basin and the adjoining marginal areas of the Ebro High. Reactivation of the Montmell Fault appears to be by some means restricted and, hence, deformation propagated to the fault footwall resulting in shortcut formation. The areas where footwall shortcut structures formed are characterized by conductive bodies at depth.

The age of the positive inversion can be relatively well established by *syn*-kinematic sediments preserved in the SE margin of the Ebro Basin. These indicate that the Gaià-El Camp Thrust emplacement is late Bartonian to lower Oligocene. The absolute age of the Montmell-Vallès Fault reactivation is uncertain. However, taking into consideration preserved pre-kinematic strata in its footwall, it can be established as, at least, late Ypresian (Cuisian).

Negative tectonic inversion of the previously formed Paleogene and Late-Jurassic faults is also within reach in the Gaià-Montmell High. During Latest Oligocene(?)/early Miocene - late Miocene extensional displacement at the SW-end of the Vallès-Penedès Fault is relayed to the Baix Penedès Fault and, at minor scale, to the Montmell Fault. Accordingly, accommodation zones characterized by the presence of relay ramp-breaching faults developed. The negative inversion of the Gaià-El amp Thrust is also identified at the NE-end of El Camp Fault, where an array of extensional faults developed in the Miramar-Gaià Domain. Tectonostratigraphic relationships indicate that extension occurred between Burdigalian and Messinian times.

The following are the supplementary data related to this article.

Declaration of Competing Interest

The authors declare that they have no known competing financial interests or personal relationships that could have appeared to influence the work reported in this paper.

Acknowledgements

This work was funded by the projects CGL2014-54118-C2-1-R/BTE MINECO/FEDER, UE; CGL2017-85532-P AEI/FEDER, UE and CGL2014-55900-P from the Spanish Ministerio de Economía y Competitividad, the project PID2019-106440GB-C21 from the Spanish Ministerio Ciencia Innovación y Universidades, the GEOMODELS Research Institute and the Grup de Geodinàmica i Anàlisi de Conques (grant no. 2017SGR-596). The authors acknowledge Schlumberger and Petroleum Experts for providing academic licenses for Dynel2D© and Move© software respectively, used in the geological mapping and structural interpretation. Constructive reviews from Christopher Connors and an anonymous reviewer significantly improved the original manuscript, for which the authors are very thankful. Ramon Carbonell is also thanked for his role as editor of the present journal.

Appendix A. Supplementary data

Supplementary data to this article can be found online at https://doi.org/10.1016/j.tecto.2021.228970.

References

Albrich, S., Bernaus, J.M., Boix, C., Caus, E., Martín-Closas, C., Salas, R., Vicedo, V., Villalonga, R., 2006. Caracterización bioestratigráfica y paleoambiental del Cretácico Inferior (Berriasiense-Barremiense) del Macizo de Garraf (Cadena Costera Catalana). Rev. Esp. Micropaleontol. 38 (2–3), 429–451.

Aldega, L., Viola, G., Casas-Sainz, A., Marcen, M., Roman-Berdiel, T., van der Lelij, R., 2019. Unraveling multiple thermotectonic events accommodated by crustal-scale faults in Northern Iberia, Spain: insights from K-Ar dating of clay gouges. Tectonics 38, 3629–3651.

Alfonso, P., Canet, C., Melgarejo, J.C., Mata-Perello, J.M., Fallick, A.E., 2012. Stable isotope geochemistry of the Ulldemolins Pb-Zn-Cu deposit (SW Catalonian Coastal Ranges, Spain). Geol. Acta 10 (2), 145–157.

Allmendinger, R., Zapata, T., Manceda, R., Dzelalija, F., 2004. Trishear kinematic modeling of structures, with examples from the Neuquen Basin, Argentina. In: McClay, K.R. (Ed.), Thrust Tectonics and Hydrocarbon Systems, AAPG Memoir, vol. 82, pp. 356–371.

Allmendinger, T., 1998. Inverse and forward numerical modeling of tri-shear fault propagation folds. Tectonics 17, 640–756.

Alonso, A., Floquet, M., Mas, R., Meléndez, A., 1993. Late cretaceous carbonate platforms: origin and evolution. Iberian Range. Spain. In: Simó, T., Scout, R.W., Masse, J.P. (Eds.), Cretaceous Carbonate Platforms, AAPG Memoir, vol. 56, pp. 297–316.

Anadón, P., 1978. El Paleógeno continental anterior a la transgresión Biarritziense (Eoceno medio) entre los ríos Gaià y Ripoll (prov. de Tarragona y Barcelona). Estud. Geol. 34, 341–440.

Anadón, P., Colombo, F., Esteban, M., Marzo, M., Robles, S., Santanach, P., Solé-Sugrañés, L., 1979. Evolución tectonoestratigráfica de los Catalánides. Acta Geol. Hispánica 14, 242–270.

Anadón, P., Cabrera, Ll, Guimerà, J., Santanach, P., 1985. Paleogene strike-slip deformation and sedimentation along the southeastern margin of the Ebro Basin. In: Biddle, K.T., Christie-Blick, N. (Eds.), Strike-Slip Deformation, Basin Formation and Sedimentation, Society of Economic Paleontologists and Mineralogists Special Publication, vol. 37, pp. 301–318.

Ashauer, H., Teichmüller, R., 1935. Die variszische und alpidische Gebirgsboldung Kataloniens. Abhandlungen Gesellschaft Wissenschaften Göttingen. Math Phys. K1 (3F), 16.

Baqués, V., Travé, A., Roca, E., Marín, M., Cantarero, I., 2012. Geofluid behaviour in successive extensional and compressional events: a case study from the southwestern end of the Vallès-Penedès Fault (Catalan Coastal Ranges, NE Spain). Pet. Geosci. 18 (2012), 17–31.
Baqués, V., Travé, A., Cantarero, I., 2013. Development of successive karstic systems within the Baix Penedès Fault zone (onshore of the Valencia Trough, NW Mediterranean). Geofluids 14, 75–94.
Barberà, X., Cabrera, L., Marzo, M., Parés, J.M., Agustí, J., 2001. A complete terrestrial Oligocene magnetobiostratigraphy from the Ebro Basin, Spain. Earth Planet. Sci. Lett. 187, 1–16.
Bartrina, M.T., Cabrera, L., Jurado, M.J., Guimerà, J., Roca, E., 1992. Evolution of the central margin of the Valencia trough (western Mediterranean). Tectonophysics 203, 219–247.
Bond, R.M.G., McClay, K.R., 1995. Inversion of lower cretaceous extensional basin, south central Pyrenees, Spain. In: Buchanan, J.G., Buchanan, P.G. (Eds.), Basin Inversion, Geological Society Special Publication, vol. 88, pp. 415–431.
Buchanan, J.G., Buchanan, P.G., 1995. Basin Inversion. Geol. Soc. Spec. Publ. 88 (596pp.).
Butler, R., Tavarnelli, E., Grasso, M., 2006. Tectonic inversion and structural inheritance in mountain belts. J. Struct. Geol. 28, 1891–1892.
Cabrera, L., Calvet, F., 1996. Onshore Neogene record in NE Spain: Vallès-Penedès and El Camp half-grabens (NW Mediterranean). In: Friend, P.T., Dabrio, D. (Eds.), Tertiary Basins of Spain, pp. 97–105.
Cabrera, L., Calvet, F., Guimerà, J., Permanyer, A., 1991. El registro sedimentario miocénico en los semigrabens del Vallès- Penedès y de El Camp: organización secuencial y relaciones tectónica sedimentación. In: I Congreso del Grupo Español del Terciario: Libro-guía Excursión, 84 (132pp.).
Cabrera, L., Roca, E., Garcés, M., de Porta, J., 2004. Estratigrafía y evolución tectonosedimentaria oligocena superior-neógena del sector central del margen catalán (Cadena Costero-Catalana). In: Vera, J.A. (Ed.), Geología de España. SGE-IGME, Madrid, pp. 569–573.
Calvert, A., Sandvol, E., Seber, D., Barazangi, M., Roecker, S., Mourabit, T., Vidal, F., Alguacil, G., Jabour, N., 2000. Geodynamic evolution of the lithosphere and upper mantle beneath the Alboran region of the western Mediterranean: constraints from travel time tomography. J. Geophys. Res. Solid Earth 105, 10871–10898.
Calvet, F., Marzo, M., 1994. El Triásico de las Cordilleras Costero Catalanas: estratigrafía, sedimentología y análisis secuencia. In: Field guide III Coloquio de Estratigrafía y Sedimentología del Triásico y Pérmico de España, pp. 1–53.
Campanyà, J., Ledo, J., Queralt, P., Marcuello, A., Muñoz, J.A., Liesa, M., Jones, A.G., 2018. New geoelectrical characterization of a continental collision zone in the Central – E astern Pyrenees: constraints from 3-D joint inversion of electromagnetic data. Tectonophysics 742-743, 168–179.
Canet, C., Alfonso, P., Melgarejo, J.C., Fallick, A.E., 2005. Stable isotope geochemistry of the carboniferous Zn-Pb-Cu sediment-hosted sulfide deposits, Northeastern Spain. Int. Geol. Rev. 47, 1298–1315.
Cantarero, I., Travé, A., Alías, G., Baqués, V., 2014. Polyphasic hydrothermal and meteoric fluid regimes during the growth of a segmented fault involving crystalline and carbonate rocks (Barcelona Plain, NE Spain). Geofluids 14, 20–44.
Cardellach, E., Canals, A., Tritlla, J., 1990. Late and post-Hercynian low temperature veins in the Catalonian Coastal Ranges. Acta Geol. Hispán. 25 (1–2), 75–81.
Carminati, E., Wortel, M.J.R., Meijer, P.T., Sabadini, R., 1998. The two-stage opening of the western-Central Mediterranean basins: a forward modeling test to a new evolutionary model. Earth Planet. Sci. Lett. 160, 667–679.
Casas, A., Permanyer, A., 1991. Disposición y estructura del zócalo de la depresión terciaria del Penedés. Rev. Inst. Investig.Geol. 35 (1891/82), 23–30.
Colombo, F., 1986. Continental Paleogene stratigraphy and sedimentology of the western southern border of the Catalanides, Tarragona Province, Spain. Cuadern. Geol. Ibérica 10, 55–115.
Cooper, M.A., Williams, G.D., de Granciasnky, P.C., Murphy, R.W., Needham, T., de Paor, D., Stonley, R., Todd, S.P., Turner, J.P., Ziegler, P.A., 1989. Inversion Tectonics – A discussion. In: Cooper, M.A., Williams, G.D. (Eds.), Inversion Tectonics, Special Publication of the Geological Society of London, vol. 44. Blackwell Scientific Publications, pp. 335–347.
Coward, M.P., 1994. Inversion tectonics. In: Hancock, P.L. (Ed.), Continental Deformation. Pergamon, Oxford, pp. 289–304.
Dahlstrom, C.D.A., 1969. Balanced cross sections. Can. J. Earth Sci. 6, 743–757.
Dañobeitia, J.J., Arguedas, M., Gallart, F., Banda, E., Makris, J., 1992. Deep crustal configuration of the Valencia Trough and its Iberian and Balearic borders from extensive refraction and wide-angle reflection profiling. Tectonophysics 203, 37–55.
Egbert, G.D., Booker, J.R., 1986. Robust estimation of geomagnetic transfer functions. Geophys. J. Int. 87, 173–194.
Enrique, P., Solé, J., 2004. El basamento ígneo. Las rocas intrusivas de la Cordillera Costero-Catalana. In: Vera, J.A. (Ed.), Geología de España. SGE-IGME, Madrid, pp. 481–484.
Escudero-Mozo, M.J., Márquez-Aliaga, A., Goy, A., Martín-Chivelet, J., López-Gómez, J., Márquez, L., Arche, A., Plasencia, P., Pla, C., Marzo, M., Sánchez-Fernández, D., 2017. Middle Triassic carbonate platforms in eastern Iberia: Evolution of their fauna and palaeogeographic significance in the western Tethys. Palaeogeogr. Palaeoclimatol. Palaeoecol. 417, 236–260.
Esteban, M., Robles, S., 1976. Sobre la paleogeografía del Cretácico Inferior de los Catalánides entre Barcelona y Tortosa. Acta Geol. Hispán. XI, 73–78.
Etheve, N., Mohn, G., Frizon de Lamotte, D., Roca, E., Tugend, J., Gómez-Romeu, J., 2018. Extreme Mesozoic crustal thinning in the Eastern Iberia margin: the example of the Columbrets Basin (Valencia Trough). Tectonics 37-2, 636–662.
Fernàndez, M., Torné, M., Zeyen, H., 1990. Lithospheric thermal structure of NE Spain and the North-Balearic Basin. J. Geodyn. 12, 253–267.
Ferrer, J., 1971. El Paleoceno y Eoceno del borde suroriental de la Depresión del Ebro (Cataluña). In: Memories Suisses de Paléontologie, 90 (70pp.).
Ferrer, O., McClay, K.R., Sellier, N.C., 2016. Influence of fault geometries and mechanical anisotropies on the growth and inversion of hanging-wall synclinal basins: insights from sandbox models and natural examples. Geol. Soc. Lond., Spec. Publ. 439, 487–509.
Fontboté, J.M., 1954. Las relaciones tectónicas de la depresión del Vallés-Penedés con la Cordillera Prelitoral Catalana y con la Depresión del Ebro. In: Tomo Homenaje a Prof. E. Hernández-Pacheco. Real Sociedad Española de Historia Natural, Madrid, pp. 281–310.
Fossen, H., Rotevatn, A., 2016. Fault linkage and relay structures in extensional settings - a review. Earth-Sci. Rev. 154, 14–28.
Galán-Abellán, B., López-Gómez, J., Berrenechea, J.F., Marzo, M., De la Horra, R., Arche, A., 2013. The beginning of the Buntsandstein cycle (Early–Middle Triassic) in the Catalan Ranges, NE Spain: Sedimentary and palaeogeographic implications. Sediment. Geol. 296, 86–102.
Gallart, F., 1981. Neógeno superior y Cuaternario del Penedés (Catalunya, España). Acta Geol. Hispán. 16, 151–157.
García-Senz, J., 2002. Cuencas extensivas del Cretácico Inferior en los Pirineos centrales. In: Formación y subsecuente inversión. Universitat de Barcelona. Ph.D. Thesis. (310pp.).
García-Senz, J., Pedrera, A., Ayala, C., Ruiz-Constán, A., Robador, A., Rodríguez-Fernández, L.R., 2019. Inversion of the north Iberian hyperextended margin: the role of exhumed mantle indentation during continental collision. Geol. Soc. Spec. Publ. 490, 177–198.
Gaspar-Escribano, J., García-Castellanos, D., Roca, E., Cloetingh, S., 2004. Cenozoic vertical motions of the Catalan Coastal Ranges (NE Spain): the role of tectonics, isostasy, and surface transport. Tectonics 23, 1–18.
Gillcrist, R., Coward, M.P., Mugnier, J.L., 1987. Structural inversion and its controls: examples from the Alpine foreland and the French Alps. Geodin. Acta 1, 5–34.
Gómez, M., Guimerà, J., 1999. Estructura Alpina de la Serra de Miramar y del NE de las Muntanyes de Prades (Cadena Costera Catalana). Rev. Soc. Geol. Esp. 12 (3–4), 405–418.
Guimerà, 2018. Structure of an intraplate fold-and-thrust belt: the Iberian Chain. A synthesis. Geol. Acta 16-4, 427–438.
Guimerà, J., 1984. Paleogene evolution of deformation in the northeastern Iberian Peninsula. Geol. Mag. 121, 413–420.
Guimerà, J., 2004. La Cadena Costera Catalana. In: Vera, J.A. (Ed.), Geología de España. SGE-IGME, Madrid, pp. 603–605.
Guimerà, J., Álvaro, M., 1990. Structure et évolution de la compression alpine dans la Chaîne ibérique et la Chaîne côtière catalane (Espagne). Bull. Soc. Géol. France 6 (2), 339–348.
Guimerà, J., Santanach, P., 1978. Sobre la compresión alpina en el sector central de las Cadenas Costeras Catalanas. Acta Geol. Hispán. 2 (13), 33–42.
Guimerà, J., Alonso, A., Mas, J.R., 1995. Inversion of an extensional-ramp basin by a newly formed thrust: The Cameros basin (N. Spain). In: Buchanan, J.G., Buchanan, P. G. (Eds.), Basin Inversion, Geological Society Special Publication, vol. 88, pp. 433–453.
Hernández, E., Casas, A., 1985. Estudio gravimétrico de la depresión del Penedés. Acta Geol. Hispán. 20 (3–4), 191–198.
Horváth, F., Berckhemer, H., 1982. Mediterranean backarc basins. In: Berckhemer, H., Hsü, K. (Eds.), Alpine Mediterranean Geodynamics, American Geophysical Union, Geodynamic Series A, vol. 7, pp. 141–173.
Jackson, J.A., 1980. Reactivation of basement faults and crustal shortening in orogenic belts. Nature 283, 343–346.
Juez-Larré, J., Andriessen, P.A.M., 2006. Tectonothermal evolution of the northeastern margin of Iberia since the break-up of Pangea to present, revealed by low-temperature fission-track and (U-Th)/He thermochronology. A case history of the Catalan Coastal Ranges. Earth Planet. Sci. Lett. 243, 159–180.
Julivert, M., 1955. Geología de la Sierra de Miramar. Memor. Comunicac. Inst. Geol. 13, 79–118.
Julivert, M., Durán, H., 1990. The Hercynian structure of the Catalonian Coastal Ranges (NE Spain). Acta Geol. Hispán. 25 (1–2), 13–21.
Lanaja, J.M., 1987. Contribución de la explotación petrolífera al conocimiento de la geología de España. IGME, Madrid.
Ledo, J., 2005. 2-D versus 3-D magnetotelluric data interpretation. Surv. Geophys. 26-5, 511–543.
Ledo, J., Queralt, P., Pous, J., 1998. Effects of galvanic distortion on magnetotelluric data over three-dimensional regional structure. Geophys. J. Int. 132, 295–301.
Llopis-Lladó, N., 1947. Contribución al conocimiento de la morfoestructura de los Catalánides. Inst. "Lucas Madalla", Barcelona CSIC (373pp.).
López-Blanco, M., Marzo, M., Burbank, D.W., Vergés, J., Roca, E., Anadón, P., Piña, J., 2000. Tectonic and climatic controls on the development of foreland fan deltas: Montserrat and Sant Llorenç del Munt systems (Middle Eocene, Ebro Basin, NE Spain). Sediment. Geol. 138, 17–39.
Marcén, M., Casas-Sainz, A.M., Román-Berdiel, T., Griera, A., Santanach, P., Pocoví, A., Gil-Imaz, A., Aldega, L., Izquierdo-Llavall, E., 2018. Multiple movements recorded in a crustal weakness zone in NE Iberia: the Vallès-Penedès Fault revisited. J. Geodyn. 121, 96–114.
Marín, M.A., Roca, E., Rosell, O., Marcuello, A., Cabrera, L., 2008. La Falla del Montmell: un ejemplo del control ejercido por las fallas extensivas mesozoicas en la arquitectura cenozoica de las Cadenas Costaneras Catalanas. Geotemas 10, 461–464.
Martí, A., Queralt, P., Roca, E., Ledo, J., Galindo-Zaldívar, J., 2009a. Geodynamic implications for the formation of the Betic-Rif orogen from magnetotelluric studies. J. Geophys. Res. 114-B1, 1–14.

Martí, A., Queralt, P., Ledo, J., 2009b. WALDIM: a code for the dimensionality analysis of magnetotelluric data using the rotational invariants of the magnetotelluric tensor. Comput. Geosci. 35 (12), 2295–2303.
Martí, A., Queralt, P., Marcuello, A., Ledo, J., Rodríguez-Escudero, E., Martínez-Díaz, J., Campanyà-Llovet, J., Meqbel, N., 2020. Magnetotelluric characterization of the Alhama de Murcia Fault (Eastern Betics, Spain) and study of magnetotelluric interstation impedance inversion. Earth Planets Space 72, 16.
Marzo, M., 1980. El Buntsandstein de los Catalánides: estratigrafía y procesos de sedimentación. PhD Thesis. Universitat de Barcelona (317pp.).
McClay, K., 1995. 2D and 3D analogue modelling of extensional fault structures; templates for seismic interpretation. Pet. Geosci. 1, 163–178.
McNeice, G.W., Jones, A.G., 2001. Multisite, multifrequency tensor decomposition of magnetotelluric data. Geophysics 66 (1), 158–173.
Melgarejo, J.C., 1987. Estudi geològic i metal·logenètic del Paleozoic del Sud de les Serralades Costaneres Catalanes.. PhD Thesis Universitat de Barcelona, pp. 1–615.
Mencos, J., Carrera, N., Muñoz, J.A., 2015. Influence of rift basin geometry on the subsequent postrift sedimentation and basin inversion: the Organyà Basin and the Bóixols thrust sheet (south central Pyrenees). Tectonics 34, 1452–1474.
Mercedes-Martín, R., Buatois, L.A., 2020. Microbialites and trace fossils from a Middle Triassic restricted carbonate ramp in the Catalan Basin, Spain: evaluating environmental and evolutionary controls in an epicontinental setting. Lethaia 54 (1), 4–25. https://doi.org/10.1111/let.12378.
Mercedes-Martín, R., Arenas, C., Salas, R., 2014. Diversity and factors controlling widespread occurrence of syn-rift Ladinian microbialites in the western Tethys (Triassic Catalan Basin, NE Spain). Sediment. Geol. 313, 68–90.
Mitra, S., Mount, V.S., 1998. Foreland-involved basement structures. Am. Assoc. Pet. Geol. Bull. 82, 70–109.
Muñoz, G., Mateus, A., Pous, J., Heise, W., Santos, F.M., Almeida, E., 2008. Unravelling middle-crust conductive layers in Palaeozoic Orogens through 3D modeling of magnetotelluric data: the Ossa-Morena Zone case study (SW Iberian Variscides). J. Geophys. Res. 113 (B06106), 1–23.
Muñoz, J.A., 1992. Evolution of a continental collision belt: ECORS-Pyrenees crustal balanced cross-section. In: McClay, K. (Ed.), Thrust Tectonics. Chapman & Hall, London, pp. 235–246.
Muñoz, J.A., 2017. Fault-related folds in the southern Pyrenees. AAPG Bull. 101-4, 579–587.
Nebot, M., Guimerà, J., 2016. Structure of an inverted basin from subsurface and field data: the Late Jurassic-Early Cretaceous Maestrat Basin (Iberian Chain). Geol. Acta 14 (2), 155–177.
Nicol, A., Watterson, J., Walsh, J.J., Childs, C., 1996. The shapes, major axis orientations and displacement patterns of fault surfaces. J. Struct. Geol. 18 (2–3), 235–248.
Ortí, F., 1974. El Keuper del Levante español. Estud. Geol. 30, 7–46.
Ortí, F., Pérez-López, A., Salvany, J.M., 2017. Triassic evaporites of Iberia: Sedimentological and palaeogeographical implications for the western Neotethys evolution during the Middle Triassic–Earliest Jurassic. Palaeogeogr. Palaeoclimatol. Palaeoecol. 471, 157–180.
Porta, J., Civís, J., 1996. La sucesión bioestratigráfica del mioceno marino en el Penedés y el horst de Tarragona-Bonastre (Neógeno del Sistema Mediterráneo). Geogaceta 19, 97–102.
Pous, J., Marcuello, A., Queralt, P., 2001. Magnetotelluric signature of the western Cantabrian Mountains. Geophys. Res. Lett. 28, 1795–1798.
Robles, S., 1982. El Cretácico de los Catalánides. In: El Cretácico de España. Universidad Complutense de Madrid, Madrid, pp. 199–272.
Roca, E., 2001. The Northwest-Mediterranean basin (Valencia Trough, Gulf of Lions and Liguro-Provencal basins): structure and geodynamic evolution. In: Ziegler, P.A., Cavazza, W., Robertson, A.H.F., Crasquin-Soleau, S. (Eds.), Peri-Tethys Memoir 6: Peri-Tethyan Rift/Wrench Basins and Passive Margins, French National Museum of Natural History, vol. 186, pp. 671–706.
Roca, E., Guimerà, J., 1992. The Neogene structure of the eastern Iberian margin: structural constraints on crustal evolution of the Valencia Trough (western Mediterranean). Tectonophysics 203, 203–218.
Roca, E., Sans, M., Cabrera, Ll, Marzo, M., 1999. Oligocene to Middle Miocene evolution of the central Catalan margin (northwestern Mediterranean). Tectonophysics 315, 209–233.
Roca, E., Frizon de Lamotte D., Mauffret, A., Bracène, R., Vergés, J., Benaouali, N., Fernández, M., Muñoz, J. A. and Zeyen, H. 2004. Transect II: Aquitaine Basin - Pyrenees - Ebro Basin - Catalan Range - Valencia Trough - Balearic Block - Algerian Basin - Kabylies - Atlas - Saharan Platform. In: Cavazza, W., Roure, F. M., Spakman, W., Stampfli, G. M. and Ziegler, P. A. (Eds.), 2004. The Transmed Atlas – The Mediterranean Region from Crust to Mantle, Springer, Berlin, Heidelberg.
Rodi, W.L., Mackie, R.L., 2001. Nonlinear conjugate gradients algorithm for 2-D magnetotelluric inversion. Geophysics 66, 174–187.
Roest, W.R., Srivastava, S.P., 1991. Kinematics of the plate boundaries between Eurasia, Iberia and Africa in the North Atlantic from the Late Cretaceous to the present. Geology 19, 613–616.
Roma, M., Ferrer, O., Roca, E., Pla, O., Escosa, F.O., Butillé, M., 2018. Formation and inversion of salt-detached ramp-syncline basins. Results from T analog modeling and application to the Columbrets Basin (Western Mediterranean). Tectonophysics 745, 214–228.
Rosenbaum, G., Lister, G.S., Duboz, C., 2002. Relative motions of Africa, Iberia and Europe during Alpine orogeny. Tectonophysics 359, 117–129.
Rubinat, M., Ledo, J., Roca, E., Rosell, O., Queralt, P., 2010. Magnetotelluric characterization of a salt diapir: a case study on Bicorb–Quesa Diapir (Prebetic Zone, SE Spain). J. Geol. Soc. 167, 145–153.
Sàbat, F., Roca, E., Muñoz, J.A., Vergés, J., Santanach, P., Sans, M., Masana, E., Estévez, A., Santisteban, C., 1997. Role of extension and compression in the evolution of eastern margin of Iberia: the ESCI-Valencia Trough seismic profile. Rev. Soc. Geol. Esp. 8 (4), 431–448.
Sáez, A., Anadón, P., 1989. El Complejo turbidítico del Carbonífero del Priorat (Tarragona). Acta Geol. Hispán. 24 (1), 33–47.
Salas, R., 1987. El Malm i el Cretaci inferior entre el Massís de Garraf i la Serra d'Espadà. Ph.D. Thesis. Universitat de Barcelona (345pp.).
Salas, R., Casas, A., 1993. Mesozoic extensional tectonics, stratigraphy and crustal evolution during the Alpine cycle of the eastern Iberian basin. Tectonophysics 228 (1–2), 33–55.
Salas, R., Guimerà, J., Mas, R., Martín-Closas, C., Meléndez, A., Alonso, A., 2001. Evolution of the Mesozoic Central Iberian Rift System and its Cainozoic inversion (Iberian Chain). In: Ziegler, P.A., Cavazza, W., Robertson, A.H.F., Crasquin-Soleau, S. (Eds.), Peri-Tethys Memoir 6: Peri-Tethyan Rift/Wrench Basins and Passive Margins, French National Museum of Natural History, vol. 186, pp. 145–185.
Salas, R., Guimerà, J., Bover-Arnal, T., Nebot, M., 2020. The Iberian-Catalan Linkage: the Maestrat and Garraf Basin. In: Quesada, Oliveira (Eds.), The Geology of Iberia: A geodynamic approach, Regional Geology Reviews, vol. 3, pp. 228–230. Ch. 5.
Serra, P.R., Enrique, P., 1989. The Late-Hercynian intrusives from southern Catalonian Coastal Ranges (NE Spain), and their epiplutonic to subvolcanic level of magma emplacement. Rend. Soc. Ital. Mineral. Petrol. 43, 817–829.
Sibuet, J.C., Srivastava, S., Spakman, W., 2004. Pyrenean orogeny and plate kinematics. J. Geophys. Res. 109, B08104.
Simpson, F., Bahr, K., 2005. Practical Magnetotellurics. Cambridge University Press (270pp.).
Srivastava, S.P., Roest, W.R., Kovacs, L.C., Oakey, G., Lévesque, S., Verhoef, J., Macnab, R., 1990. Motion of Iberia since the Late Jurassic: results from detailed aeromagnetic measurements in the Newfoundland Basin. Tectonophysics 184, 229–260.
Tugend, J., Manatschal, G., Kusznir, N.J., 2015. Spatial and temporal evolution of hyperextended rift systems: implication for the nature, kinematics, and timing of the Iberian-European plate boundary. Geology 43 (1), 15–18.
Van Hinsbergen, D.J.J., Vissers, R.L.M., Spakman, W., 2014. Origin and consequences of western Mediterranean subduction, rollback, and slab segmentation. Tectonics 33, 393–419.
Vergés, J., Fernàndez, M., Martínez, A., 2002. The Pyrenean origin: pre-, syn-, and post-collisional evolution. In: Rosenbaum, G., Lister, G.S. (Eds.), Reconstruction of the Evolution of the Alpine-Himalayan Orogen, Journal of the Virtual Explorer, vol. 8, pp. 57–76.
Vidal, N., Gallart, J., Dañobeitia, J., Díaz, J., 1995. Mapping the Moho in the Iberian Mediterranean margin by multicoverage processing and merging of wide-angle and near-vertical reflection data. In: Banda, E., Torné, M., Talwani, M. (Eds.), Rifted Ocean Continent Boundaries, NATO ASI Series C, Mathematical and Physical Sciences, vol. 463, pp. 291–308.
Virgili, C., Cassinis, G., Broutin, J., 2006. Permian to Triassic sequences from selected continental areas of Southwestern Europe. Geol. Soc. Lond. Spec. Publ. 265, 231–265.
Williams, G.D., Powell, C.M., Cooper, M.A., 1989. Geometry and kinematics of inversion tectonics. In: Cooper, M.A., Williams, G.D. (Eds.), Inversion Tectonics, Geological Society of London, Special Publication, vol. 44, pp. 3–15.
Withjack, M.O., Schlische, R.W., 2006. Geometric and experimental models of extensional fault-bend folds. In: Buiter, S.J.H., Schreurs, G. (Eds.), Analogue and Numerical Modelling of Crustal-Scale Processes, Geological Society of London, Special Publication, vol. 253, pp. 285–305.